Functional analysis of the polar amino acid in TatA transmembrane helix

Binhan Hao, Wenjie Zhou, Steven M. Theg

Plant Biology Department, University of California, Davis, CA 95616

November 30, 2021

For correspondence e-mail: smtheg@ucdavis.edu

Abstract

The twin-arginine translocation (Tat) pathway utilizes the proton-motive force (pmf) to transport folded proteins across cytoplasmic membranes in bacteria and archaea, as well as across the thylakoid membrane in plants and the inner membrane in mitochondria. In most species, the minimal components required for Tat activity consist of three subunits, TatA, TatB, and TatC. Previous studies have shown that a polar amino acid is present at the N-terminus of the TatA transmembrane helix (TMH) across many different species. In order to systematically assess the functional importance of this polar amino acid in the TatA TMH in *Escherichia coli*, a complete set of 19-amino-acid substitutions was examined. Unexpectedly, although being preferred overall, our experiments suggest that the polar amino acid is not necessary for a functional TatA. Hydrophobicity and helix stabilizing properties of this polar amino acid were found to be highly correlated with the Tat activity. Specifically, change in charge status of the amino acid side chain due to pH resulted in a shift in hydrophobicity, which was demonstrated to impact the Tat transport activity. Furthermore, a four-residue motif at the N-terminus of the TatA TMH was identified by sequence alignment. Using a biochemical approach, the N-terminal motif was found to be functionally significant, with evidence indicating a potential role in the preference for utilizing different pmf components. Taken together, these findings yield new insights into the functionality of TatA and its potential role in the Tat transport mechanism.

Introduction

The twin-arginine translocation (Tat) pathway, a protein transport machinery, is found in bacteria, archaebacteria, chloroplasts, and plant mitochondria. In bacteria, the Tat pathway is involved in many critical biological processes, including cell division, stress tolerance and electron transport (Berks, 2015; Gohlke et al., 2005; Ize et al., 2003). In plants, the Tat pathway transports several proteins that are essential for photosynthesis across thylakoid membranes (Clark and Theg, 1997). In haloarchaea which normally possess high cytoplasmic salt concentration leading to faster protein folding, the Tat pathway serves almost 50% of secretome (Ghosh et al., 2019). Unlike the similarly ubiquitous Sec pathway, the Tat pathway is able to transport folded proteins (Clark and Theg, 1997) while requiring only the proton motive force (pmf), with no contribution from NTP hydrolysis (Braun et al., 2007).

The Tat system in most species consists of three subunits, TatA, TatB, and TatC (Berks, 2015). It has been shown that all three subunits can form a complex which works as a receptor for signal peptides of Tat substrates. After the receptor complex binds to the Tat substrate, more TatA subunits are recruited to the translocon. While, TatB and TatC are present in a 1:1 stoichiometry in the complex, TatA is present at much higher stoichiometries (8-40 folds) (Leake et al., 2008; Mori et al., 2001; Sargent et al., 2001).

The structures of the three individual Tat subunits have been determined (Hu et al.,

2010; Rollauer et al., 2012; Zhang et al., 2014). Both TatA and TatB possess a short transmembrane helix (TMH) followed by a hinge region, one or more amphipathic helices (APH), and then a relatively unstructured C-terminus. Conversely, TatC has six TMHs and exhibits a cupped hand shape. Remarkably, the Tat machinery transports folded proteins of different sizes without introducing significant ion leakage (Asher and Theg, 2021; Teter and Theg, 1998). Recent work suggests that this occurs in the absence of channel/pore like structure, unlike the well-characterized Sec translocon (Tsirigotaki et al., 2017). It has been proposed that Tat pathway operates through lipid-lined toroidal pores formed in a destabilized membrane, rather than common proteinaceous pore (Asher and Theg, 2021; Brüser and Sanders, 2003).

Previous studies have demonstrated that TatAs have a highly conserved short TMH (Hao et al., 2021) which could cause membrane destabilization and is critical to the overall Tat function (Hao et al., 2021; Hou et al., 2018). Such short TMHs make the TatA protein energetically unfavorable to span on the membrane bilayer. Furthermore, it has been shown that almost all TatA family proteins contain a polar residue at the N-terminus of its TMH (Hicks et al., 2003). In *Escherichia coli* (*E. coli*), TatA has a glutamine (Q) at the 8th position (TMH: 6th – 20th), while in pea chloroplasts, TatA has a glutamic acid (E) instead at the corresponding position. A cysteine-scanning study in *E. coli* TatA illustrated that cysteine substitution for the 8th glutamine (Q8C mutant) led to the complete loss of Tat activity, whereas cysteine substitutions for all the other residues in the TMH retained Tat transport activity similar to that of the wtTatA

(Greene et al., 2007). Further studies showed that *E. coli* TatA asparagine substitution (Q8N) and Q8E mutants retained the ability to export TMAO (trimethylamine *N*-oxide) reductase (TorA) to the periplasm (Greene et al., 2007), while the alanine (Q8A) mutant was not able to transport either TorA (Greene et al., 2007) or CueO (Alcock et al., 2016). However, another study showed a somewhat conflicting result that *E. coli* Q8A and Q8C mutants retained TorA transport capability when overexpressed (Warren et al., 2009). On the other hand, in pea or maize chloroplasts, it was shown that all of the 10th glutamic acid substitution variants, E10A, E10D, and E10Q, severely affected Tat transport in a biochemical complementation assay (Dabney-Smith et al., 2003; Fincher et al., 2003). Interestingly, although the chloroplast TatA E10Q mutant exhibited extremely low Tat activity, the *E. coli* TatA Q8E mutant displayed high Tat transport activity, suggesting that residue preference was not identical for different species. Furthermore, the *Bacillus subtilis* Tat system contains two sets of TatA/TatC subunits (TatAd/TatCd and TatAy/TatCy), and those TatAs actually lack this “conserved” polar residue in the TMH. Although extensive effort has been made to investigate the function of this “conserved” polar amino acid in TatA, the lack of a complete set of mutants and use of different transport assays has allowed the role of this residue at the analogous position to remain an open question.

In this study, we analyzed the amino acid requirement for the 8th residue in *E. coli* TatA through a complete set of Q8 mutants. Both qualitative and quantitative assays were conducted to compare the activity between TatA mutants. Unexpectedly, we

found that polar amino acids were preferred overall but actually not necessary for a functional TatA. However, the Tat activity was highly correlated with hydrophobicity and helix stability of the 8th residue in TatA. Furthermore, by sequence alignment and biochemical analysis, a four-residue motif at the N-terminus of the TatA TMH was found to be functionally significant. These results expand our understanding of the potential function of TatA and provide new insight into the Tat transport mechanism.

Results

1. Polar amino acids at the 8th position in *E. coli* TatA TMH are preferred but not necessary for minimal Tat activity.

To systematically assess the characteristic requirements of the 8th residue in *E. coli* TatA, Q8 was replaced by all the other 19 amino acids and their effects on Tat activity was measured. Membrane stability of TatA Q8 mutants was assessed by membrane isolation followed by carbonate wash, and all mutants displayed an integrated presence in the membrane (Supplemental figure 1). Minimal Tat activity was subsequently screened by SDS growth assays (Ize et al., 2003) for each of the TatA Q8 mutants. All polar amino acid substitutions (Q8N, Q8S, Q8T, Q8D, Q8E, Q8H, Q8K, and Q8R) exhibited sufficient Tat activity to grow in LB medium containing 10% SDS (Figure 1A). Surprisingly, TatA Q8A, Q8C, Q8G, and Q8P mutants, whose substituted amino acids do not possess strong polar side chains, also showed a growth activity in the same medium (Figure 1B, C). The rest of substitutions (Q8F, Q8I, Q8L, Q8M, Q8V, Q8W, and Q8Y) displayed no growth activity in LB medium containing 5% SDS, indicating a complete loss of Tat activity (Figure 1C). An *in vivo* transport assay was implemented to further confirm the SDS growth assay result. In this assay, a FLAG-tagged *E. coli* native Tat substrate, SufI-FLAG, was overexpressed in the TatA Q8 mutants. After 2.5 hours transport at 37°C, a periplasmic fraction was isolated by treated with EDTA/lysozyme and osmatic shock (Petiti et al., 2017a), a harsh method that minimizes the loss of periplasmic proteins. The precursor and mature forms of SufI-FLAG were

separated by SDS-PAGE according to their size. This assay revealed that, despite their ability to grow in 10% SDS, the Q8A, Q8C, Q8D, Q8E, Q8G, Q8P, Q8R, and Q8T mutants displayed significant significantly lower Tat activity (<25%) compared to wild-type TatA (Figure 1D).

Pulse-chase assays, representing a more fine-grained assessment of Tat transport activity (Palmer et al., 2010), was conducted (at 37°C and pH = 7.0), were conducted with all the functional TatA Q8 mutants to compare their transport rates. Figure 2A shows the quantitative analysis of the pulse chase results (Supplemental figure 2). An exponential plateau model $y = y_{\max} - (y_{\max} - y_0) \times e^{-kt}$ was applied in data fitting. Estimated initial transport rate (V_0) derived from the fitting curve was used to compare the transport activity between the TatA Q8 mutants (Figure 2B). Unexpectedly, the Q8H mutant exhibited the highest V_0 (228% of the V_0[wtTatA]). Q8N, Q8S, and Q8E variants of TatA, exhibited 58%, 37% and 33% of the V_0[wtTatA], respectively. However, Q8A, Q8C, Q8D, Q8G, Q8K, Q8P and Q8R showed relatively lower transport rate (less than 25% of V_0[wtTatA]). One unanticipated finding was that the Q8T, Q8D and Q8R mutants, whose 8th glutamine was replaced by a polar amino acid, showed even lower transport rates than the poorly performing Q8A mutant. The results from pulse-chase assays were overall consistent with the *in vivo* transport assay except that Q8K performed relatively worse in the pulse-chase assay than in the *in vivo* transport assay.

In summary, polar amino acids are overall strongly favored at the 8th position in the *E. coli* TatA but not necessary for a functional Tat translocon. Moreover, not all polar amino acid substitutions showed higher transport ability than non-polar substitutions.

2. The Tat activity of Q8 mutants is correlated with the side chain hydrophobicity and helix stabilizing properties of the substituted amino acid.

Our data clearly show that polar amino acids are preferred overall in the TatA 8th position, but are not strictly necessary to retain Tat activity (ex. Q8A, Q8C, Q8G, Q8P). Moreover, some of the polar residue substitutions (i.e., Q8D, Q8R and Q8T), even though they retained the minimal Tat activity required to grow in LB medium with SDS, displayed significantly lowered transport activity. Such results could not simply be explained by the binary categories, polar or non-polar, of amino acids. In order to understand the functional importance of this position in the *E. coli* TatA, a further analysis of the amino acids' preference is needed. On one hand, previous studies showed that the overall hydrophobicity of the TatA TMH might affect TatA function in thylakoids (Hauer et al., 2017). On the other, a recent study has demonstrated that the hydrophobic mismatch between the TatA TMH and membrane bilayer is critical to Tat function (Hao et al., 2021; Mehner-Breitfeld et al., 2021). To maintain such a hydrophobic mismatch, a relatively stable alpha helix structure is likely to be required.

To assess these properties, the hydrophobicity and α-helix stability of each amino acid (Monera et al., 1995) were plotted together with the transport performance of the corresponding TatA Q8 mutants (Figure 1E). Interestingly, a high correlation between Tat activity and the combination of hydrophobicity and α-helix stability was observed: 1) the Q8 mutants which completely lost Tat activity clustered at the top-right corner, suggesting that very high hydrophobicity and helix stability at this position are detrimental for Tat transport. 2) all mutants with high Tat activity were clustered in the middle ranges of hydrophobicity and helix stability (Figure 1E, pink box). These observations draw our attention to the importance of a moderate hydrophobicity and α-helix stability of the 8th amino acid in *E. coli* TatA.

3. Charge status of the side chain of the polar amino acid affects the TatA function.

Due to the nature of polar amino acids with electrically charged side chains, previous studies have reported that the hydrophobicity of those amino acids changes dramatically under different pH conditions (Kovacs et al., 2006; Mant and Hodges, 2002). For instance, the side chain of histidine ($pKa_{(His)} = 6.04$) is relatively hydrophobic (similar as Ala) at pH 7 (mostly uncharged), while it becomes one of the most hydrophilic side chains when the pH is lower than 5 (mostly charged). In this study, we hypothesized that a moderately hydrophobic side chain is required for the 8th residue in the *E. coli*

TatA. To further investigate this hypothesis, a comparison of Tat transport rates between wtTatA and Q8H was studied under different pH conditions. The pulse-chase experiments in Figure 2 showed that the Q8H mutant performed approximately 2-fold better than the wild-type TatA at pH = 7.0 where most of (90%) the histidines in TatAs were presumably deprotonated. To assess whether a change in histidine hydrophobicity would alter activity of the Q8H mutant, we measured transport rates by pulse-chase at pH 5.0, 6.0 and 8.0 (Figure 3A). Figure 3 shows that wtTatA and Q8H had different behaviors when transporting SufI at different pH. First, wtTatA and Q8H mutant exhibited optimal transport rates at different pH values (Figure 3B and C). wtTatA displayed optimal transport activity at pH 5.0, while the optimal pH for Q8H mutant was 7.0. However, their highest V_0 values were comparable to each other (Figure 3D). Second, V_0[wtTatA] was significantly higher than V_0[Q8H] at pH = 5.0 (Figure 3E) whilst V_0[wtTatA] was significantly lower than V_0[Q8H] at pH = 7.0 (Figure 3G). Third, wtTatA had a very similar V_0 as Q8H mutant at pH = 8.0 (Figure 3H) where 99% of the histidines were presumably deprotonated, a similar status as uncharged glutamine in wtTatA. In summary, the charged status of the histidine side chain, a model residue for comparison with the wtTatA, affects its transport.

In the aggregate, our experiments in the pH range 5.0-8.0 are consistent with the hypothesis that a functional Tat translocon requires that its TatA possesses a moderately hydrophobic amino acid at 8th position. In addition, it demonstrates that not only hydrophobicity of different amino acid but also hydrophobicity of same amino acids

under different charged status affects its ability to support Tat transport. Together these results provide important insights into understanding the function of the 8th residue in *E. coli* TatA (see discussion).

To further investigate how charged residues in TatA affect the overall Tat transport machinery, we determined how well the membrane can hold a pmf by measuring the ΔpH induced by ATP hydrolysis in inverted membrane vesicles (IMVs) membrane expressing corresponding mutated TatA proteins. According to their charge status at pH 7.0, Q8E, wtTatA, Q8H and Q8K mutants were selected as examples of negatively, neutral, partially positively and completely positively charged residues at the 8th position in *E. coli* TatA (Figure 4A). wtTatA and the Q8E mutant showed similar low membrane leakage outcomes in the presence or absence of the TatBC complex. However, Q8H and Q8K mutants exhibited significant different membrane leakage characteristics when the TatBC complex was present. Q8H, which showed the highest membrane leakage without TatBC, displayed less membrane leakage when TatBC was also expressed on the membrane. In contrast, the Q8K mutant showed the opposite behavior, exhibiting the highest ΔpH without TatBC but developing a dramatically high membrane leak when TatBC was present. That is to say, even though lysine and glutamic acid have similar hydrophobicity at pH 7.0 (Figure 1E), their different charge status might affect how they interact with the TatBC complex, which results in different membrane leakage outcomes. The cause for this behavior is not clear and awaits further investigation.

4. Different species have different preferences for polar amino acids in the TatA TMH.

Even though in *E. coli* TatA, the polar amino acid in the TMH is the uncharged glutamine, in plant, the Tat system, this position is usually occupied by a glutamic acid, a charged amino acid (Mori and Cline, 2001). Moreover, *Bacillus subtilis*, a gram-positive bacterium, expresses two different kinds of TatA with glycine (TatAc) or serine (TatAy) at the corresponding position. To investigate if such amino acid choices are correlated to species, TatA sequences were aligned according to five categories: proteobacteria (N=7534), actinobacteria and firmicutes (N=6978), chloroplasts (N=242), cyanobacteria (N=149) and archaea (N=151). A conserved 12-residue hydrophobic core was observed (9th – 20th in Figure 5A-E) before the invariant "FG" motif at the end of TMH (Hao et al., 2021). In addition, there is a clear preference for particular amino acids in the TatA TMH at the 8th position with different species (Figure 5F) (Here, we use the numbering from *E. coli* for simplicity. The exact number might be different in different species.) In proteobacteria (representing *E. coli*), histidine (50%) and glutamine (34%) are the top two choices. Interestingly, such choice preferences are consistent with our Tat activity results in that Q8H and wtTatA exhibited the highest Tat transport rates. In contrast, in the other two groups of bacteria, actinobacteria and firmicutes, even though histidine is still the top choice for TatA (46%), glutamine is present in only 2% of the species in these categories, and relatively more of them choose

glutamic acid (32%) or glycine (10%) compared to proteobacteria. However, all of chloroplasts, cyanobacteria and archaea TatAs have a highly conserved glutamic acid (>90%) at the 8th position. Remarkably, even though polar amino acids are present in TatA in most species, 1% of actinobacteria and firmicutes (N = 80) and 0.1% of proteobacteria (N = 13) possesses an alanine at that position. This finding further confirms our experimental observations that polar residues at 8th position are not indispensable for a functional TatA (Supplemental Figure 3A and B). Such different preferences in different species suggest that a possible evolutionary pressure exists at this position for the Tat pathway to accommodate various external conditions.

5. A four-residues functional motif at the N-terminus of the TatA TMH is important for Tat activity.

Besides the various preference of amino acids at the 8th position in different species, a conserved GxPE motif (the 5th to 8th position in Figure 5C, D and E) was also observed in chloroplasts, cyanobacteria, and archaea TatAs. In contrast, in proteobacteria, actinobacteria and firmicutes, such “GxPE” motif was not obviously presented. Instead, a SIW(H/Q) motif was generally conserved in proteobacteria. To see if these motifs are correlated to different polar amino acids, TatA sequences were further examined based on the identity of the amino acid at the 8th position (Supplemental Figure 3). Supplemental Figure 3A clearly shows that proteobacteria favor “SIWH” and “SIWQ”

(i.e., *E. coli*) at the N-terminus of the TatA TMH. In addition, "GLPG", "SITK" and "S(I/L)WN" motifs were identified in proteobacteria as well. Interestingly, in *E. coli* TatE, "SITK" was at the corresponding location (the 5th to 8th residues). It has been reported that the TatE gene was found only in enterobacteria, a subset of proteobacteria (Yen et al., 2002). Accordingly, in this study, TatA or TatE sequences from enterobacteria were also aligned (Supplemental Figure 3F) to check if such motifs are also present in other TatE genes. Surprisingly, "SIWQ" and "SITK" were extremely conserved across TatA (N=599) and TatE (N=160), respectively, in enterobacteria. Additionally, although "SIWH" was the most conserved motif in proteobacteria, gram-positive bacteria favored "xPWH" in the same position (Supplemental Figure 3B), These results suggest that the four-residues motif at the N-terminus of the TatA TMH might play an important role in TatA function despite minor deviations in different species.

To assess whether the corresponding four-residue motifs are required for specific amino acids at the 8th position to exhibit higher Tat transport activity, we also substituted the 5th to 8th amino acids in *E. coli* TatA according to the above conserved motifs, including "GVPE" (a motif of chloroplasts TatAs), "GLPE" (a motif of cyanobacteria TatAs) and "SITK" (a motif of enterobacteria TatEs). Moreover, to comprehensively understand how the 5th to 7th amino acids affects TatA function, the 5th to 8th residues of *E. coli* TatA were also changed to "GVPQ" or "GLPQ" (Figure 6).

308 A recent study has shown that a shorter TMH negatively affects TatA's membrane
309 stability (Hao et al., 2021). In terms of our new mutants, GVP(E/Q) and GLP(E/Q), it
310 is possible that those mutants lost their ability to stably embed into the membrane since
311 proline (immediately before the 8th residue) usually acts as a helix breaker (Chou and
312 Fasman, 1978) in protein secondary structure. Figure 6A shows that TatA in GVP(E/Q)
313 and GLP(E/Q) mutants exhibited much lower membrane abundance compared to
314 wtTatA or Q8E mutant, indicating that a proline residue severely affects the membrane
315 insertion, even though it did not cause high membrane leakage in those mutants (Figure
316 4B and C). But, very surprisingly, GVPE mutant displayed a better performance than
317 Q8E in the *in vivo* transport assay (Figure 6B). Pulse-chase assays with those N-motif
318 mutants were also conducted to quantitatively compare their transport rates. Both
319 GLPQ and GVPQ displayed somewhat lower transport rates than wtTatA, suggesting
320 that a disruption of the conserved "SIWQ" motif was deleterious to *E. coli* TatA
321 function (Figure 6C). However, GVPE and SITK mutants exhibited significantly higher
322 transport rates than Q8E and Q8K mutants, respectively, which indicates that the
323 evolutional conserved motifs are functionally more suitable for certain amino acids at
324 the 8th position in TatA (Figure 6D-F). In spite of that replacing to conserved N-motifs
325 were generally beneficial for Tat function, we also observed that the GLPE mutant
326 supported significantly lower transport rates than both the GVPE and Q8E mutants.
327 Such results demonstrate that changes of a single amino acid in the N-terminal motif
328 (even from one hydrophobic residue to another hydrophobic residue) strongly affected
329 the final TatA function. This confirms our hypothesis that the N-terminus of TatA, and

not just the well-known polar amino acid, determines the Tat transport activity. Further, it implies that the combinations of these amino acids at the N-terminus of the TatA TMH are potentially tuned to their own membrane environments, and those different motifs could be a strategy to adjust to diverse and subtle biological membrane properties.

6. The conserved "GVPE" motif from chloroplast TatA might be responsible for preference of utilization of ΔpH.

Even though the GVPE mutant performed significantly better than the Q8E mutant (Figure 6F), it was still less effective than the wild-type SIWQ motif in the *E. coli* TatA. This result does not point to an explanation of why most chloroplasts and cyanobacteria possess a glutamic acid at the 8th position in their TatAs. It was previously shown that the chloroplast Tat system is highly dependent on ΔpH (Cline et al., 1992), while *E. coli* Tat system does not require ΔpH for active transport (Bageshwar and Musser, 2007a). These energetic preferences are also consistent with their own respective tendencies to partition their pmfs between a ΔpH and a Δψ (Cruz et al., 2001; Zilberstein et al., 1984). To investigate if the invariant motif in chloroplast TatA is related to this energetic preference, IMVs, the bacterial counterpart to chloroplast thylakoids, were made from wtTatA, Q8E and GVPE mutants. A previous study (Bageshwar and Musser, 2007a) used IMVs to test Tat transport ability powered by different components of the pmf. In our hands also, the IMVs made with wild-type *E. coli* Tat displayed a higher transport

ability in the presence of nigericin which presumably dissipated the ΔpH. Figure 7A shows that wtTatA and the Q8E mutant displayed consistently higher performance in the presence of nigericin. However, the GVPE mutant exhibited significantly lower transport capability when the ΔpH was dissipated. These results suggest that GVPE mutant relied more on ΔpH for transport than the wtTatA or the Q8E mutant.

Discussion

An incomplete set of *E. coli* TatA Q8 mutants was a limitation to further understand the function of the overall "conserved" polar amino acid in TatA TMH. In this study, we systematically analyzed the transport ability of all the Q8 mutants which the 8th glutamine of *E. coli* TatA was substituted by the rest of 19 amino acids. Three assays were conducted to compare the transport rates between different mutants, qualitatively and quantitatively. The transport ability results of our TatA Q8 mutants showed that a polar amino acid at the 8th position of TatA is preferred but not necessary for a functional TatA (Figure 1 and 2). Furthermore, a strong correlation between Tat transport activity and hydrophobicity and helix stability of the 8th residue was noticed based on our experimental results (Figure 1E). It reveals that a residue with moderate range of hydrophobicity and helix stability was preferred for TatA to retain high transport ability. Moreover, by altering the environmental pH in our transport assay, we demonstrated that Q8H mutant, a basic amino acid substitution, exhibited significantly lower transport ability under charged status of the 8th residues where the hydrophobicity of the corresponding residue becomes much lower than the hypothesized required range (Figure 3). Furthermore, by analyzing the alignments of TatA sequences, we found that different species have different preferred amino acids at the 8th position and a conserved 4-residue motif at the N-terminus of TMH was identified corresponding to different 8th residue in TatA sequences (Figure 5). Such 4-residue motif located at the N-terminus of TatA TMH was further tested in *E. coli* TatA and proved to have significant positive effect on the transport ability (Figure 6). Additionally, such motif was shown to be

relevant to the preference for usage of ΔpH or ΔΨ component of pmf (Figure 7).

These results, together, provides some new perspectives to understand the functional requirement of the 8th residue in TatAs.

First, the hydrophobicity, but not polarity of the 8th amino acid, is critical for TatA. It supports the idea that the 8th residue's ability to respond membrane potential or electrically interact with other polar amino acids in other Tat subunits is not necessary for the fundamental transport mechanism. Additionally, since *E. coli* TatA lacks a charged polar amino acid, but chloroplasts TatA has a charged residue, at the corresponding position, it has been discussed that bacteria and thylakoids might use different mechanisms in terms of TatA function (New et al., 2018). It has been debated if the active shift of protonation states of the glutamic acid in the chloroplasts TatA is required to be functional (Berks, 2015; New et al., 2018). According to our data, a possible explanation for this might be that the pKa of the side chain of glutamic acid matches the thylakoids lumen pH (Kramer et al., 1999) and changes the overall hydrophobicity of glutamic acid (Kovacs et al., 2006) on the chloroplasts TatAs to the moderate range. Such explanation could be further supported by two indirect evidence. On one hand, it has been showed that, in thylakoids Tat transport, there was a delay between the light illumination and transport event (a sigmoidal transport curve). Such delay could be attributed to the delayed pH changes in thylakoids lumen after the light illumination (Cruz et al., 2001; Davis et al., 2017). That is to say, the lumen pH is not

low enough to fulfill the requirement of hydrophobicity of glutamic acid immediately after the illumination. The thylakoids Tat pathway is not fully activated after a long dark treatment when the lumen pH is high. On the other hand, in our sequence alignments result, it shows that a few archaea species have TatAs with an aspartic acid (Supplemental Figure 3E) at the corresponding position whose side chain's pKa is even lower than glutamic acid. By analyzing the living pH for those species, interestingly, all of them were found to live in an extreme acidic environment (Supplemental Table 1). Such observations give an example of how Tat system might be altered to accommodate to different environmental conditions.

Second, it indicates that the ability to create a relatively unstable N-terminus structure is significant for the 8th residue in TatA TMH. Theoretically, such residue, which has a side chain of low hydrophobicity and locates at the contacting surface between lipid hydrophobic core and aqueous environment, keeps the potential ability to energetically overcome the hydrophobic effect (between TatA transmembrane and lipid acyl chains) and get access to aqueous environment (Rodriguez et al., 2013). Meanwhile, previous literature reported that *E. coli* TatA TMH is tuned to be 15-residue long to keep the hydrophobic mismatch while maintain membrane integrity to have the best Tat transport activity. Also, it has been shown that TatAs have a highly conserved 12-residue long hydrophobic core (9th-20th in *E. coli* TatA) in the TMH (Hao et al., 2021). Those factors make the segment of TatA TMH buried in the lipids could be as short as 12 amino acids when the 8th residue is exposed to the aqueous environment, transiently.

Thus, the membrane bilayer might rupture (or form pore) due to the too short hydrophobic segment and transport event occurs. Our data demonstrated that if the 8th residue, in opposite, had very high hydrophobicity (Figure 1E), Tat transport was completely blocked although the hydrophobic mismatch between TatA TMH and membrane bilayer was still maintained. It suggests that a 15-residue long TMH is required but insufficient for active Tat transport. However, a transition from 15-residue to even shorter TMH perhaps matters.

Third, we showed that not only the 8th residue is critical, but also the amino acids combination of N-terminus of TatA TMH affects the overall TatA function (Figure 5 and 6). A 4-residue motif at the N-terminus of TatA TMH was identified in this study. Such result was not revealed by previous studies for two reasons. First, such functional N-terminus motif was not obviously conserved across different species. For example, in chloroplasts and cyanobacteria, “GxPE” motif was nearly invariant at the N-terminus of TatA TMH. However, this motif was not observed in other bacteria species. Second, such N-terminus motif showed strong correlation with the 8th residue in the TatA TMH. For instance, in proteobacteria, “SIW” was conserved from 5th to 7th position when the 8th residue was glutamine or histidine whereas such combination was not shown when lysine or glycine was at the 8th position (Supplemental Figure 3). Even though we still do not understand the explicit role of those conserved motif, the amino acid choices in those motifs could give us some clues about the function of N-terminus of TatA TMH. First, a tryptophan was observed immediately before histidine or glutamine in

446 proteobacteria and other two groups of gram-positive bacteria. One question would be
447 what are the special features of tryptophan that make it very conserved in TatA TMH.
448 Tryptophan is normally considered as a non-polar amino acid in biochemistry. However,
449 it possesses one of the most polarizable side chains, the indole group. Such feature
450 makes tryptophan highly abundant at the water-lipid interface and usually works as an
451 anchor to stabilize membrane protein (de Jesus and Allen, 2013; Sun et al., 2008).
452 Moreover, the indole group could response to electric field and reach the lowest energy
453 state when it is aligned with the force lines of electric field (Zhang and Li, 2019). So,
454 the tryptophan might help TatA embed in the membrane and anchor its position near
455 the interface. Second, we noticed that a proline residue is highly conserved immediately
456 before the glutamic acid in TatAs. Prolines are generally considered as a breaker in
457 alpha-helix of soluble proteins (Barlow and Thornton, 1988). However, several
458 literatures reported that proline would not disrupt the alpha-helix structure in the
459 membrane environment (Li et al., 1996; Senes et al., 2004). Moreover, it has been
460 shown that the hinge-bending motions of proline residue are likely to play a significant
461 role in catalysis and signal transduction (S.P. Sansom and Weinstein, 2000; Tieleman et
462 al., 2001). Such possible function to create a temporary hinge at the N-terminus of TatA
463 TMH is consistent with our hypothesis that a transition to even shorter TMH is
464 significant for Tat mechanism. In addition, according to TatA NMR structure (Hu et al.,
465 2010), such 4-residue motif presents at the first round of TMH. Ser6 and Gln8 orientate
466 oppositely than Ile6 and Trp7, suggesting a local amphipathic topology. Moreover,
467 other 4-residues motifs in chloroplasts or gram-positive bacteria also follow this rule

468 even though they have different combinations of 4 residues at those positions.

469

470 Based on our new understanding of the function of TatA subunits, in this study, we
471 would like to propose a new model for the mechanism of Tat pathway (Figure 8). (i)
472 Before substrate binding, TatA, TatB and TatC form an oligomer structure, which severs
473 as the receptor complex for signal peptide of Tat substrates(Alcock et al., 2016). Under
474 this stage, only a few TatA proteins get involved in the translocon. (ii) – (iii) After
475 binding to substrate, the receptor complex gets a conformation change and attract more
476 TatA proteins to the receptor complex (Aldridge et al., 2014) with the help with pmf.
477 Unlike a conventional proposed ring-like structure for TatA oligomers, here, by the
478 inspiration of a recent paper (Mehner-Breitfeld et al., 2021), we propose that more TatA
479 proteins will be recruited into a two-layers line manner at the first place. (iv) As more
480 TatA proteins get recruited to the translocon, both hydrophobic mismatch effect and
481 unstable N-terminus structure give the potential to break up the two-layers TatA line,
482 drag other Tat subunits apart, and form a toroidal pore (v). (vi) After substrates getting
483 through the pore, Tat subunits will go back to the original state (similar structure as (i)).
484 However, since the receptor complex goes back to resting state, excess TatAs go back
485 to membrane and wait for a new round of recruitment.

486

487 In this study, although we analyzed the functional requirements of the 8th residue in *E.*
488 *coli* TatA, such results might not be directly applicable to all other species. For example,
489 it is possible that chloroplasts TatA could not tolerate a wide range of amino acids

substitution at the corresponding position as *E. coli* TatA since the lumen pH is relatively low and, unlike *E. coli*, ΔΨ is not the dominant component of thylakoid pmf. Besides, in some species, there is no TatB presence in their Tat system. Due to bifunction of their TatAs, it is possible that the TatA/TatC system has more restrictions at the 8th residue in TatA.

Methods

1. Strain and Plasmid Constructions

E. coli strain DADE-A (MC4100, *ΔtatABCE*, arabinose resistance) was used in this study (Wexler et al., 2000). For TatA variants in pTat101 (Kneuper et al., 2012), a low copy plasmid expressing the TatABC constitutively, the corresponding single and multiple substitutions were introduced by QuickChange site-directed mutagenesis (NEB, Phusion High-Fidelity PCR Kit) followed by KLD (Kinase, Ligase, and DpnI) digestion (NEB). Detailed primers used for TatA variant construction can be found in Supplemental Table 2. For TatA variants in pBAD22, a vector with arabinose-inducible *araBAD* operon, indicated TatA alleles, together with the wild-type TatBC, were amplified from the respective constructs in pTat101. For TatA single Q8 substitution, forward primer TatA_gopBAD22_F (5'-ACCACAGAGGAACATGTATGGGTGGTA TCAGTATTTG-3') was used. For TatA multiple substitutions, forward primer TatAnmotif_gopBAD22_F (5'- CTACCACAGAGGAACATGTATGGGTGGTATC-3') was used. Reverse primer TatABC_gopBAD22_R (5'-TCTAGAGGCGGTTGAAT TTATTCTTCAGTTTTTTCGC-3') was used in both cases. Empty vectors were constructed using the primers pBAD22delABC_F (5'-ATTCAACCGCCTCTAGAG-3') and pBAD22delABC_R (5'-ACATGTTCCTCTGTGGTAG-3'). Fragments and vector were assembled using Gibson Assembly approach (NEBuilder HiFi DNA Assembly Master Mix). For TatA variants in pBAD33, a vector with arabinose-inducible *araBAD* operon, 6X His tag was first added at the C-terminal of TatA by using the primers pBAD33His_F (5'- CATCATCATCACCACCACTAATGGC-3') and

pBAD33His_R (5'-TGATGATGACCCACCTGCTCTTTATCGTG-3'). Subsequently, TatA mutations were introduced by QuickChange site-directed mutagenesis mentioned above. pQE80l (SufI-FLAG) for the *in vivo* transport assay was constructed as describe previously (Huang and Palmer, 2017). pNR14 and pNR42, two plasmids used in pulse chase experiments, were as described previously (Sargent et al., 1999; Stanley et al., 2000). All plasmids were confirmed by Sanger sequencing. Detailed information in plasmid constructions can be found in Supplemental Table 3.

2. Sequence Alignments and Statistical Analyses

A total of 15054 TatA sequences were downloaded from the identical protein groups in GenBank (NCBI).Sequences were then subset into five groups based on taxonomy (7534 from proteobacteria, 6978 from firmicutes and actinobacteria, 149 from cyanobacteria, 242 from chloroplast, and 151 from archaea), which were subsequently subjected to multiple sequence alignments within each group using MAFFT (Rozewicki et al., 2019). Sequence logos corresponding to each group were generated using RStudio (Ver. 1.4.1103) with ggseqlogo package (Wagih, 2017). For the interest of this project, sequences were further grouped by the identity of the residue aligned to the eighth position in *E. coli* TatA, and the corresponding sequence logos were generated. Further, a stacked bar chart summarizing the distribution of the identity of residues in this position in each taxonomical group was plotted using GraphPad Prism version 8.2.1 for Windows (GraphPad Software, San Diego, California USA).

3. Liquid SDS Growth Assay

Overnight bacteria cultures were sub-cultured with an optical density (OD_{600}) of 0.002 were grown in the Luria-Bertani (LB) medium containing 0%, 5%, or 10% SDS, respectively. After cells were incubated at 37°C with shaking for 5 hours, the final OD_{600} were measured. For each mutant, survival ratio was calculated by its final OD_{600} at the indicated SDS concentration to the final OD_{600} in the LB medium without SDS.

4. *in vivo* Transport Assay and Cell Fractionation

Corresponding mutant plasmids derived from pTat101 were co-transformed with pQE80l (SufI-FLAG), which under the control of the T5 promoter, into the DADE-A strain. Overnight cultures were diluted in a fresh LB medium at a ratio of 1:100 and grown at 37 °C until the OD_{600} reached 0.5. A final concentration of 1 mM IPTG (isopropyl β-D-1-thiogalactopyranoside) was added to induce the expression of SufI-FLAG. After cultured at 37°C for another 2.5 hours, 3 mL of the cells with an OD_{600} equivalent to 1 were fractionated using the EDTA/lysozyme/cold osmotic shock method described before (Petiti et al., 2017b). Periplasmic fractions were collected by adding equal volume of 2X SDS sample buffer, which were then subjected to SDS-PAGE. Membrane fractions were washed in 10 mM Na_2CO_3 for 1 hour at 4°C with gentle shaking. Subsequently, samples were ultracentrifuged at 120,000 x g for 45 min at 4°C. Pellets were resuspended with 2X SDS sample buffer and collected as the membrane fractions.

5. SDS-PAGE and Western Blot

For periplasmic fractions, samples were immunoblotted with α-FLAG (GenScript) followed by HRP-conjugated α-mouse antibodies (Santa Cruz Biotechnology). For membrane fractions, after transfer the proteins to the PVDF membranes, PVDF membranes were cut and immunoblotted with α-TatA and α-TatB antibodies respectively followed by HRP-conjugated α-rabbit antibody (GenScript). Proteins were visualized using ProSignal Pico ECL Western Blotting detection kit (Genesee Scientific).

6. Pulse-Chase Experiment and Autoradiography

The pulse-chase experiment protocol was modified from (Stanley et al., 2000). Tat variants carrying pNR14 and pNR42 were grown overnight in LB media at 30°C, which were then sub-cultured in fresh LB media the next day for 1.5 hours at 30°C. Subsequently, cells were harvested and normalized to the equivalent of 0.5 mL cells with OD_{600} = 0.2. Cells were washed with 0.5 mL 1X M9 medium (diluted from 10X M9 medium supplemented with 0.1 mM $CaCl_2$, 0.002% thiamine, 2 mM $MgSO_4$, and 0.01% of the 18 amino acids excluding methionine and cysteine, pH = 7.0). Cells were resuspended in 2.5 mL M9 medium and cultured for another hour at 30°C. Then, cells were transferred to 42°C for 15 min to induce T7 polymerase from pNR42. 400 μg/mL of rifampicin was added to inhibit the *E. coli* endogenous RNA polymerase, and cells were grown at 42°C for another 10 min. Subsequently, cells were grown at 30°C for another 20 mins before transferred to the indicated temperature until the completion of

the experiment. If needed, pH was adjusted by 1 M HCl or 1 M KOH immediately after this step. Bacteria cultures were then incubated at indicated temperature for 5 min. 0.025 mCi of [^{35}S] methionine (PerkinElmer Inc. NEG772002MC) was added for the pulse step, and 750 μg/mL of unlabeled cold methionine was added after 5 min. 300 μL of the culture was taken at the indicated time point, and transport was quenched by freezing in liquid nitrogen. Samples were subsequently thawed on ice, centrifuge, and resuspended with 2X SDS sample buffer followed by SDS-PAGE and autoradiography. Results were quantified using ImageJ software.

7. Statistical Analysis of the Pulse-Chase Experimental Results

Mature-to-total (sum of precursor and mature) data from the pulse-chase experiment was plotted against each time point, which were then fitted with the exponential plateau model deriving from the first-order reaction model, $y = (y_{max} - y_0) \times e^{-kt}$, using GraphPad Prism. y_{max} was defined as the maximum of the mature-to-total value, and y_0 represents the initial mature-to-total value at the end of the pulse. t represents time in minutes. the initial velocity (V_0), representing the transport rate when $y = 0$, was obtained by $V_0 = y_{max} \times k$, with the units of the reciprocal minutes.

8. IMVs (Inverted-Membrane Vesicles) preparation

Tat proteins expression and IMVs preparation were performed as described (Bageshwar and Musser, 2007b), with the following modifications. Cells were resuspended with the

same lysis buffer as described, which were then passed through a French press at ~ 6000 psi once. Subsequently, cells were centrifuged at 30,000 g for 20 mins at 4°C. Supernatants were then centrifuged at 140,000 g for 1 hr. Pellets were resuspended with IMV storage buffer (10 mM Tris-HCl, pH = 7.5, 1 mM $MgSO_4$, 1 mM KCl, 40% glycerol). IMVs were stored in -80°C freezer.

9. Proton Leakage Measurement

IMVs were made from the DADE-A cells expressing the 6X His-tagged wild-type or TatA variants in pBAD33 alone or together with the pTat101(*ΔtatA*). Acridine orange fluorescence-quenching assays were carried out using the Fluorolog-3 spectrofluorometer (HORIBA Scientific, model No. FL3-22). IMVs were added to the final concentration equivalent to A_{280} = 0.375 to the reaction mix containing 1X TE buffer (25 mM MOPS, 25 mM MES, 5 mM $MgCl_2$, 50 mM KCl, 200 mM sucrose, and 57 μg/mL BSA, pH = 7.0), ATP regeneration system (2.9 mM phosphocreatine, 0.29 mg/mL creatine kinase), and 2 μM acridine orange. The reaction mix was incubated for 5 mins with gentle stirring at 37°C before measurement. The fluorescence of acridine orange was recorded at λ_{ex} = 494 nm (slit = 1 nm) and λ_{em} = 540 nm (slit = 5 nm) per 0.1 second. 4 mM of ATP was added at 60 seconds, and 10 μM of CCCP was added at 200 seconds to dissipate the proton gradient.

Acknowledgement

We gratefully acknowledge support from the Division of Chemical Sciences, Geosciences, and Biosciences, Office of Basic Energy Sciences of the U.S. Department of Energy through Grant DE-SC0020304 to SMT.

References

Alcock F, Stansfeld PJ, Basit H, Habersetzer J, Baker MA, Palmer T, Wallace MI, Berks BC. 2016. Assembling the Tat protein translocase. *eLife* **5**:e20718. doi:10.7554/eLife.20718

Aldridge C, Ma X, Gerard F, Cline K. 2014. Substrate-gated docking of pore subunit Tha4 in the TatC cavity initiates Tat translocase assembly. *J Cell Biol* **205**:51–65. doi:10.1083/jcb.201311057

Asher AH, Theg SM. 2021. Electrochromic shift supports the membrane destabilization model of Tat-mediated transport and shows ion leakage during Sec transport. *Proc Natl Acad Sci U S A* **118**. doi:10.1073/pnas.2018122118

Bageshwar UK, Musser SM. 2007a. Two electrical potential–dependent steps are required for transport by the Escherichia coli Tat machinery. *J Cell Biol* **179**:87–99. doi:10.1083/jcb.200702082

Bageshwar UK, Musser SM. 2007b. Two electrical potential-dependent steps are required for transport by the Escherichia coli Tat machinery. *J Cell Biol* **179**:87–99. doi:10.1083/jcb.200702082

Barlow DJ, Thornton JM. 1988. Helix geometry in proteins. *J Mol Biol* **201**:601–619. doi:10.1016/0022-2836(88)90641-9

Berks BC. 2015. The Twin-Arginine Protein Translocation Pathway. *Annu Rev Biochem* **84**:843–864. doi:10.1146/annurev-biochem-060614-034251

Braun NA, Davis AW, Theg SM. 2007. The Chloroplast Tat Pathway Utilizes the Transmembrane Electric Potential as an Energy Source. *Biophys J* **93**:1993–1998. doi:10.1529/biophysj.106.098731

Brüser T, Sanders C. 2003. An alternative model of the twin arginine translocation system. *Microbiol Res* **158**:7–17. doi:10.1078/0944-5013-00176

Chou PY, Fasman GD. 1978. Empirical Predictions of Protein Conformation. *Annu Rev Biochem* **47**:251–276. doi:10.1146/annurev.bi.47.070178.001343

Clark SA, Theg SM. 1997. A folded protein can be transported across the chloroplast envelope and thylakoid membranes. *Mol Biol Cell* **8**:923–934. doi:10.1091/mbc.8.5.923

Cline K, Ettinger WF, Theg SM. 1992. Protein-specific energy requirements for protein transport across or into thylakoid membranes. Two lumenal proteins are transported in the absence of ATP. *J Biol Chem* **267**:2688–2696.

Cruz JA, Sacksteder CA, Kanazawa A, Kramer DM. 2001. Contribution of Electric Field (Δψ) to Steady-State Transthylakoid Proton Motive Force (pmf) in Vitro and in Vivo. Control of pmf Parsing into Δψ and ΔpH by Ionic Strength. *Biochemistry* **40**:1226–1237. doi:10.1021/bi0018741

Dabney-Smith C, Mori H, Cline K. 2003. Requirement of a Tha4-conserved Transmembrane Glutamate in Thylakoid Tat Translocase Assembly Revealed by Biochemical Complementation. *J Biol Chem* **278**:43027–43033. doi:10.1074/jbc.M307923200

Davis GA, Rutherford AW, Kramer DM. 2017. Hacking the thylakoid proton motive force for improved photosynthesis: modulating ion flux rates that control proton

motive force partitioning into Δψ and ΔpH. *Philos Trans R Soc B Biol Sci* **372**:20160381. doi:10.1098/rstb.2016.0381

de Jesus AJ, Allen TW. 2013. The role of tryptophan side chains in membrane protein anchoring and hydrophobic mismatch. *Biochim Biophys Acta BBA - Biomembr* **1828**:864–876. doi:10.1016/j.bbamem.2012.09.009

Fincher V, Dabney-Smith C, Cline K. 2003. Functional assembly of thylakoid ΔpH-dependent/Tat protein transport pathway components in vitro. *Eur J Biochem* **270**:4930–4941. doi:10.1046/j.1432-1033.2003.03894.x

Ghosh D, Boral D, Vankudoth KR, Ramasamy S. 2019. Analysis of haloarchaeal twin-arginine translocase pathway reveals the diversity of the machineries. *Heliyon* **5**:e01587. doi:10.1016/j.heliyon.2019.e01587

Gohlke U, Pullan L, McDevitt CA, Porcelli I, Leeuw E de, Palmer T, Saibil HR, Berks BC. 2005. The TatA component of the twin-arginine protein transport system forms channel complexes of variable diameter. *Proc Natl Acad Sci* **102**:10482–10486. doi:10.1073/pnas.0503558102

Greene NP, Porcelli I, Buchanan G, Hicks MG, Schermann SM, Palmer T, Berks BC. 2007. Cysteine Scanning Mutagenesis and Disulfide Mapping Studies of the TatA Component of the Bacterial Twin Arginine Translocase. *J Biol Chem* **282**:23937–23945. doi:10.1074/jbc.M702972200

Hao B, Zhou W, Theg SM. 2021. Hydrophobic mismatch effect is a key factor in protein transport on the Tat pathway. *bioRxiv* 2021.05.26.445883. doi:10.1101/2021.05.26.445883

Hauer RS, Freudl R, Dittmar J, Jakob M, Klösgen RB. 2017. How to achieve Tat transport with alien TatA. *Sci Rep* **7**:1–13. doi:10.1038/s41598-017-08818-w

Hicks MG, Leeuw E de, Porcelli I, Buchanan G, Berks BC, Palmer T. 2003. The Escherichia coli twin-arginine translocase: conserved residues of TatA and TatB family components involved in protein transport. *FEBS Lett* **539**:61–67. doi:10.1016/S0014-5793(03)00198-4

Hou B, Heidrich ES, Mehner-Breitfeld D, Brüser T. 2018. The TatA component of the twin-arginine translocation system locally weakens the cytoplasmic membrane of Escherichia coli upon protein substrate binding. *J Biol Chem* **293**:7592–7605. doi:10.1074/jbc.RA118.002205

Hu Y, Zhao E, Li H, Xia B, Jin C. 2010. Solution NMR Structure of the TatA Component of the Twin-Arginine Protein Transport System from Gram-Positive Bacterium Bacillus subtilis. *J Am Chem Soc* **132**:15942–15944. doi:10.1021/ja1053785

Huang Q, Palmer T. 2017. Signal Peptide Hydrophobicity Modulates Interaction with the Twin-Arginine Translocase. *mBio* **8**:e00909-17. doi:10.1128/mBio.00909-17

Ize B, Stanley NR, Buchanan G, Palmer T. 2003. Role of the Escherichia coli Tat pathway in outer membrane integrity. *Mol Microbiol* **48**:1183–1193. doi:10.1046/j.1365-2958.2003.03504.x

Kneuper H, Maldonado B, Jäger F, Krehenbrink M, Buchanan G, Keller R, Müller M, Berks BC, Palmer T. 2012. Molecular dissection of TatC defines critical regions

718 essential for protein transport and a TatB–TatC contact site. *Mol Microbiol*
719 **85**:945–961. doi:10.1111/j.1365-2958.2012.08151.x
720 Kovacs JM, Mant CT, Hodges RS. 2006. Determination of intrinsic
721 hydrophilicity/hydrophobicity of amino acid side chains in peptides in the
722 absence of nearest-neighbor or conformational effects. *Pept Sci* **84**:283–297.
723 doi:https://doi.org/10.1002/bip.20417
724 Kramer DM, Sacksteder CA, Cruz JA. 1999. How acidic is the lumen? *Photosynth Res*
725 **60**:151–163. doi:10.1023/A:1006212014787
726 Leake MC, Greene NP, Godun RM, Granjon T, Buchanan G, Chen S, Berry RM, Palmer
727 T, Berks BC. 2008. Variable stoichiometry of the TatA component of the twin-
728 arginine protein transport system observed by in vivo single-molecule imaging.
729 *Proc Natl Acad Sci* **105**:15376–15381. doi:10.1073/pnas.0806338105
730 Li SC, Goto NK, Williams KA, Deber CM. 1996. Alpha-helical, but not beta-sheet,
731 propensity of proline is determined by peptide environment. *Proc Natl Acad Sci*
732 **93**:6676–6681. doi:10.1073/pnas.93.13.6676
733 Mant CT, Hodges RS. 2002. Reversed-phase liquid chromatography as a tool in the
734 determination of the hydrophilicity/hydrophobicity of amino acid side-chains at
735 a ligand–receptor interface in the presence of different aqueous environments:
736 I. Effect of varying receptor hydrophobicity. *J Chromatogr A*, 21st International
737 Symposium on the Separation of Proteins, Peptides and Polynucleotides
738 **972**:45–60. doi:10.1016/S0021-9673(02)00354-0
739 Mehner-Breitfeld D, Ringel MT, Tichy DA, Endter LJ, Stroh KS, Luensdorf H,
740 Risselada HJ, Brueser T. 2021. TatA and TatB generate a hydrophobic mismatch
741 that is important for function and assembly of the Tat translocon in Escherichia
742 coli. *bioRxiv* 2021.05.26.445790. doi:10.1101/2021.05.26.445790
743 Mori H, Cline K. 2001. Post-translational protein translocation into thylakoids by the
744 Sec and ΔpH-dependent pathways. *Biochim Biophys Acta BBA - Mol Cell Res*
745 **1541**:80–90. doi:10.1016/S0167-4889(01)00150-1
746 Mori H, Summer EJ, Cline K. 2001. Chloroplast TatC plays a direct role in thylakoid
747 ΔpH-dependent protein transport. *FEBS Lett* **501**:65–68. doi:10.1016/S0014-
748 5793(01)02626-6
749 New CP, Ma Q, Dabney-Smith C. 2018. Routing of thylakoid lumen proteins by the
750 chloroplast twin arginine transport pathway. *Photosynth Res* **138**:289–301.
751 doi:10.1007/s11120-018-0567-z
752 Palmer T, Berks BC, Sargent F. 2010. Analysis of Tat Targeting Function and Twin-
753 Arginine Signal Peptide Activity in Escherichia coli In: Economou A, editor.
754 Protein Secretion: Methods and Protocols, Methods in Molecular Biology.
755 Totowa, NJ: Humana Press. pp. 191–216. doi:10.1007/978-1-60327-412-8_12
756 Petiti M, Houot L, Duché D. 2017a. Cell Fractionation In: Journet L, Cascales E, editors.
757 Bacterial Protein Secretion Systems: Methods and Protocols, Methods in
758 Molecular Biology. New York, NY: Springer New York. pp. 59–64.
759 doi:10.1007/978-1-4939-7033-9_3
760 Petiti M, Houot L, Duché D. 2017b. Cell Fractionation In: Journet L, Cascales E, editors.
761 Bacterial Protein Secretion Systems: Methods and Protocols, Methods in

Molecular Biology. New York, NY: Springer. pp. 59–64. doi:10.1007/978-1-4939-7033-9_3

Rodriguez F, Rouse SL, Tait CE, Harmer J, Riso AD, Timmel CR, Sansom MSP, Berks BC, Schnell JR. 2013. Structural model for the protein-translocating element of the twin-arginine transport system. *Proc Natl Acad Sci* **110**:E1092–E1101. doi:10.1073/pnas.1219486110

Rollauer SE, Tarry MJ, Graham JE, Jääskeläinen M, Jäger F, Johnson S, Krehenbrink M, Liu S-M, Lukey MJ, Marcoux J, McDowell MA, Rodriguez F, Roversi P, Stansfeld PJ, Robinson CV, Sansom MSP, Palmer T, Högbom M, Berks BC, Lea SM. 2012. Structure of the TatC core of the twin-arginine protein transport system. *Nature* **492**:210–214. doi:10.1038/nature11683

Rozewicki J, Li S, Amada KM, Standley DM, Katoh K. 2019. MAFFT-DASH: integrated protein sequence and structural alignment. *Nucleic Acids Res* **47**:W5–W10. doi:10.1093/nar/gkz342

Sargent F, Gohlke U, Leeuw E de, Stanley NR, Palmer T, Saibil HR, Berks BC. 2001. Purified components of the Escherichia coli Tat protein transport system form a double-layered ring structure. *Eur J Biochem* **268**:3361–3367. doi:10.1046/j.1432-1327.2001.02263.x

Sargent F, Stanley NR, Berks BC, Palmer T. 1999. Sec-independent Protein Translocation in Escherichia coli. *J Biol Chem* **274**:36073–36082. doi:10.1074/jbc.274.51.36073

Senes A, Engel DE, DeGrado WF. 2004. Folding of helical membrane proteins: the role of polar, GxxxG-like and proline motifs. *Curr Opin Struct Biol* **14**:465–479. doi:10.1016/j.sbi.2004.07.007

S.P. Sansom M, Weinstein H. 2000. Hinges, swivels and switches: the role of prolines in signalling via transmembrane α-helices. *Trends Pharmacol Sci* **21**:445–451. doi:10.1016/S0165-6147(00)01553-4

Stanley NR, Palmer T, Berks BC. 2000. The twin arginine consensus motif of Tat signal peptides is involved in Sec-independent protein targeting in Escherichia coli. *J Biol Chem* **275**:11591–11596. doi:10.1074/jbc.275.16.11591

Sun H, Greathouse DV, Andersen OS, Koeppe RE. 2008. The Preference of Tryptophan for Membrane Interfaces. *J Biol Chem* **283**:22233–22243. doi:10.1074/jbc.M802074200

Teter SA, Theg SM. 1998. Energy-transducing thylakoid membranes remain highly impermeable to ions during protein translocation. *Proc Natl Acad Sci* **95**:1590–1594. doi:10.1073/pnas.95.4.1590

Tieleman DP, Shrivastava IH, Ulmschneider MR, Sansom MSP. 2001. Proline-induced hinges in transmembrane helices: Possible roles in ion channel gating. *Proteins Struct Funct Bioinforma* **44**:63–72. doi:10.1002/prot.1073

Tsirigotaki A, De Geyter J, Šoštaric´ N, Economou A, Karamanou S. 2017. Protein export through the bacterial Sec pathway. *Nat Rev Microbiol* **15**:21–36. doi:10.1038/nrmicro.2016.161

Wagih O. 2017. ggseqlogo: a versatile R package for drawing sequence logos. *Bioinformatics* **33**:3645–3647. doi:10.1093/bioinformatics/btx469

Warren G, Oates J, Robinson C, Dixon AM. 2009. Contributions of the Transmembrane Domain and a Key Acidic Motif to Assembly and Function of the TatA Complex. *J Mol Biol* **388**:122–132. doi:10.1016/j.jmb.2009.02.060

Wexler M, Sargent F, Jack RL, Stanley NR, Bogsch EG, Robinson C, Berks BC, Palmer T. 2000. TatD is a cytoplasmic protein with DNase activity. No requirement for TatD family proteins in sec-independent protein export. *J Biol Chem* **275**:16717–16722. doi:10.1074/jbc.M000800200

Yen M-R, Tseng Y-H, Nguyen EH, Wu L-F, Saier MH. 2002. Sequence and phylogenetic analyses of the twin-arginine targeting (Tat) protein export system. *Arch Microbiol* **177**:441–450. doi:10.1007/s00203-002-0408-4

Zhang XC, Li H. 2019. Interplay between the electrostatic membrane potential and conformational changes in membrane proteins. *Protein Sci* **28**:502–512. doi:10.1002/pro.3563

Zhang Y, Wang L, Hu Y, Jin C. 2014. Solution structure of the TatB component of the twin-arginine translocation system. *Biochim Biophys Acta BBA - Biomembr* **1838**:1881–1888. doi:10.1016/j.bbamem.2014.03.015

Zilberstein D, Agmon V, Schuldiner S, Padan E. 1984. Escherichia coli intracellular pH, membrane potential, and cell growth. *J Bacteriol* **158**:246–252.

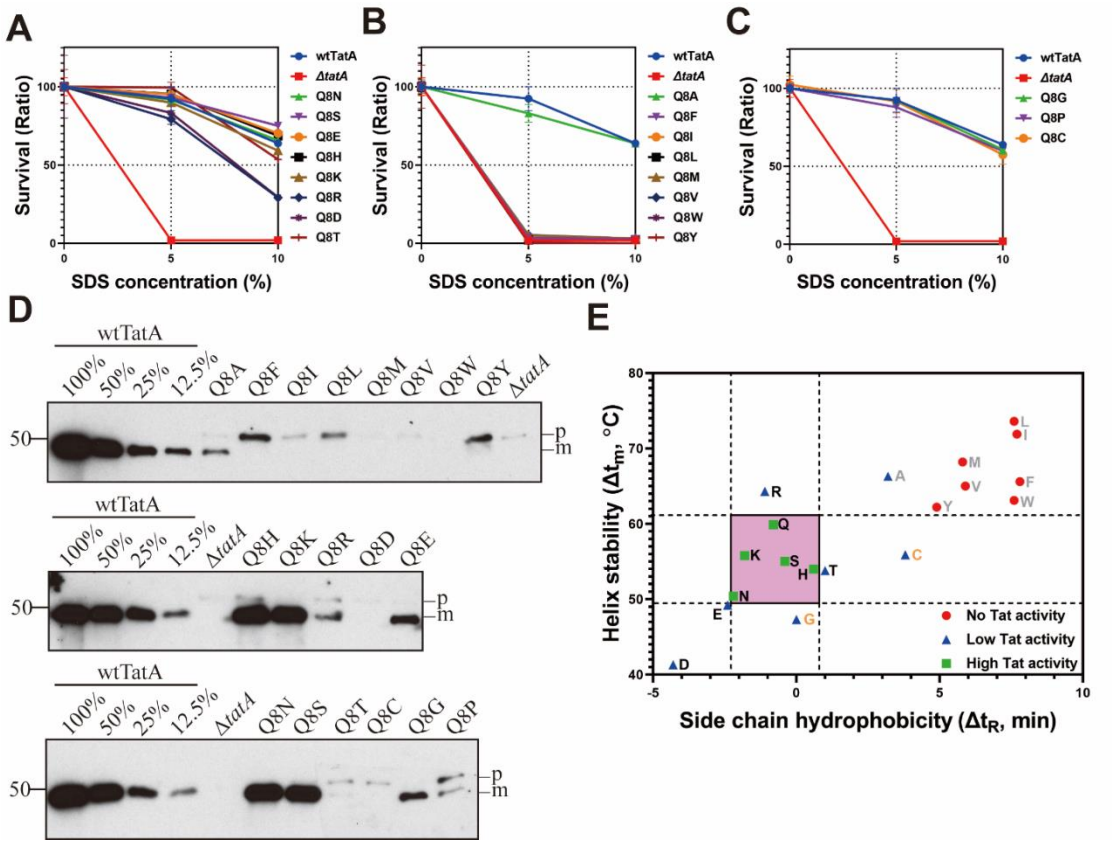

Figure 1. Polar residues at the eighth position of the *E. coli* TatA TMH are preferred but not necessary for minimal Tat activity. (A-C) Minimal Tat transport abilities of the TatA Q8 variants were evaluated by the growth performance in the LB medium with indicated SDS concentration. wtTatA served as the positive control, while *ΔtatA* acted as the negative control. Survival ratio denotes the ratio of the OD_{600} of the cells grown in the presence of the corresponding SDS concentration to the OD_{600} of the cells grown without SDS. Three biological replicates for each mutant were included in the experiments. (D) Western blot results of the *in vivo* transport assays with the TatA Q8 variants. Dilutions of the amount of transported SufI-FLAG in the wtTat cells were shown for the comparison of the transport performance in the TatA Q8 variants. p, precursor and m, mature. (E) Plot of the helix stability (Δt_m) versus side chain hydrophobicity (Δt_R) of the identity of the 19 amino acids (20 amino acids except proline) regarding the Tat transport activity. Different levels of the Tat transport activities are denoted with the following rules. no Tat activity stands for no growth in the LB medium containing 5% SDS; low Tat activity stands for those mutants who could grow in the LB with SDS but showed less than 50% transport activity than wtTat in the *in vivo* transport assay in (D); and high Tat activity stands the ability to transport more than 50% than wtTat in the *in vivo* transport in (D). Identities of the amino acids with high Tat activity were clustered in the ranges of moderate helix stability and side chain hydrophobicity, which is boxed in pink.

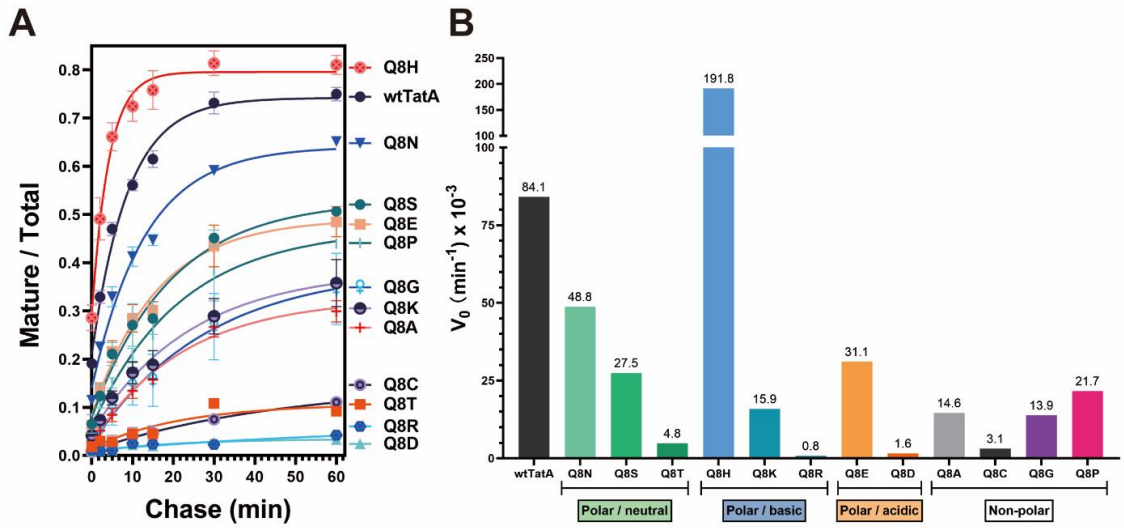

Figure 2. Quantitative analyses of the Tat activity in the TatA Q8 variants. (A) Plot of the transport kinetics of the TatA Q8 variants in pulse-chase experiment. Identities of wtTatA and TatA Q8 variants are shown in the right, accordingly. Mature/total denotes the ratio of the mature band to the sum of the precursor and mature bands in autoradiography of the samples from the pulse-chase experiment transporting SufI. Chase time is denoted on the x-axis. At least two biological replicates were included in this experiment for each mutant. Exponential plateau model was used for data fitting. (B) Plot of the initial velocities (V_0) in the TatA Q8 variants transporting SufI. Further analyses were performed based on the transport kinetics in (A).. Exact values of the V_0 are shown on top. TatA Q8 variants are grouped based on the categories of the residues.

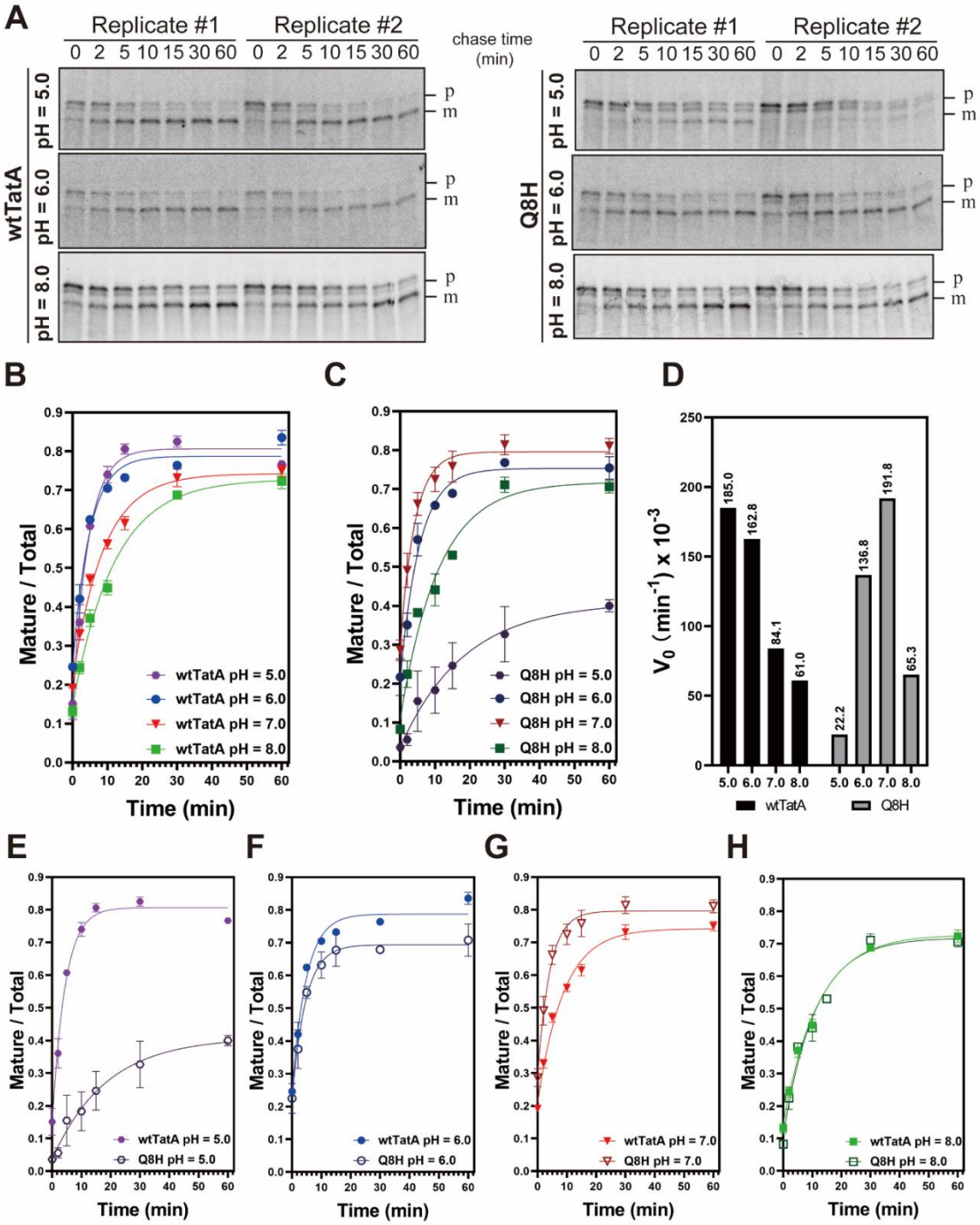

Figure 3. Comparison of the Tat activity of wtTat and Q8H mutant under different pH conditions. (A) Radioautography of the wtTatA and Q8H variants transporting SufI under different pHs. Samples from the pulse-chase experiment were subjected to SDS-PAGE. 8-16% polyacrylamide gels were used to separate the mature SufI (m) from the precursor (p). Corresponding time of chase step are shown on top. Two replicates for each variant were included in this experiment. (B-C) Quantitative analyses of the transport performance between the wtTatA (B) and Q8H (C) variants based on the radioautography in (A). Same analysis approach was used as mentioned earlier. The pH condition in which the experiment was performed is indicated in the legend of the plot. (D) Plot of the initial velocities under different pH

conditions between the wtTat and Q8H variants. Same approach was implemented as described before. Initial velocities of the wtTatA under different pH are denoted in black, and initial velocities of the Q8H variant under different pH are denoted in grey. (E-H) Comparison of the transport kinetics between the wtTatA and Q8H variants under the same pH (E, pH = 5.0; F, pH = 6.0; G, pH = 7.0; H, pH = 8.0), with the filled circles representing the wtTatA, and empty circles representing the Q8H.

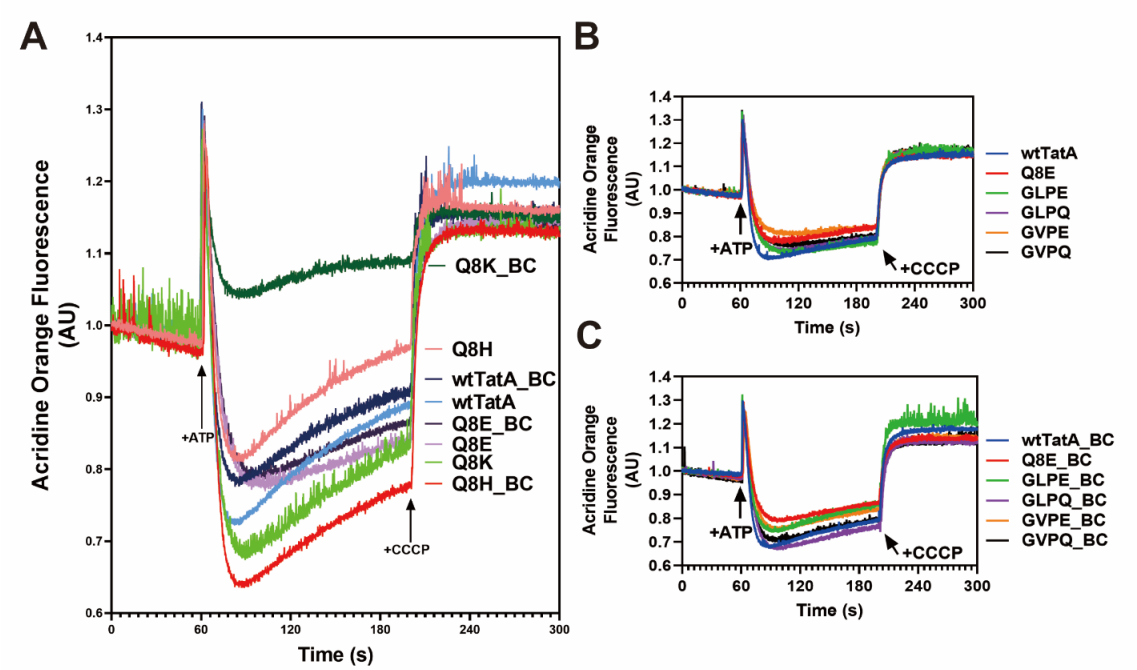

Figure 4. Membrane leakage profiles of TatA mutants. membrane stability. The ΔpH developed across the membrane was measured by the acridine orange quenching in the IMVs. 4 mM ATP was added at the 60 secs to energize the IMV, and 10 μM CCCP was added at 200 secs to dissipate the proton gradient, resulting the recovery of the fluorescence. (A) Measurement of the ΔpH in the DADE (Tat knockout variant) IMVs with indicated overexpressed TatA Q8 variants alone or together with the constitutively expressed TatBC. (B) Measurement of the ΔpH in the DADE (Tat knockout variant) IMVs with indicated overexpressed TatA N-terminal motif variants alone. (C) Measurement of the ΔpH in the DADE (Tat knockout variant) IMVs with indicated overexpressed TatA N-terminal motif variants together with the constitutively expressed TatBC. AU, arbitrary unit.

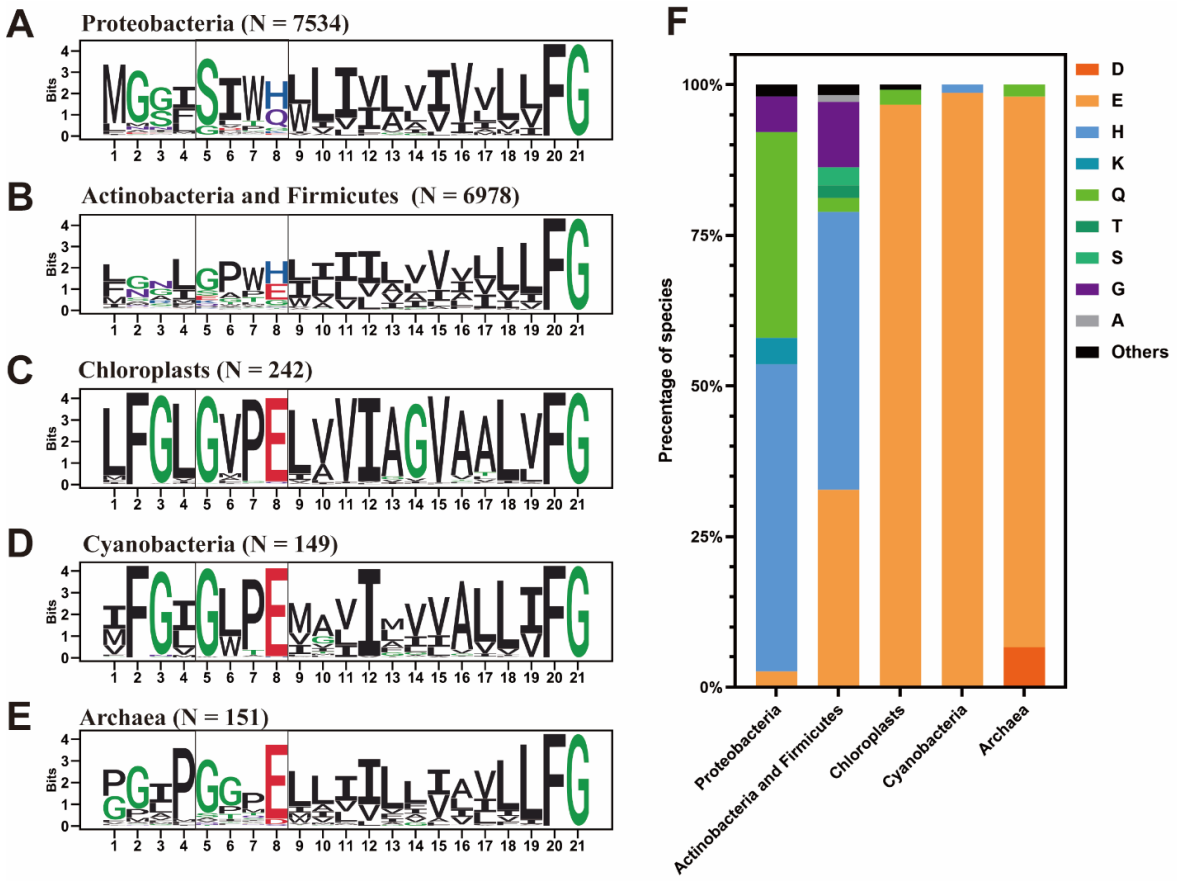

Figure 5. Different species have different preferences at 8th position in the TatA. Sequence logos of the TatA sequences alignment across (A) proteobacteria, (B) actinobacteria and firmicutes, (C) chloroplasts, (D) cyanobacteria, and (E) archaea. Numbers of sequences included in the corresponding categories were denoted as N. The N-terminal motifs were boxed as indicated. (F) Distributions of amino acids selected in the location equivalent to the 8th position of the *E. coli* TatA across different species. Percentage of species with the indicated residues were shown. Amino acids were colored as indicated.

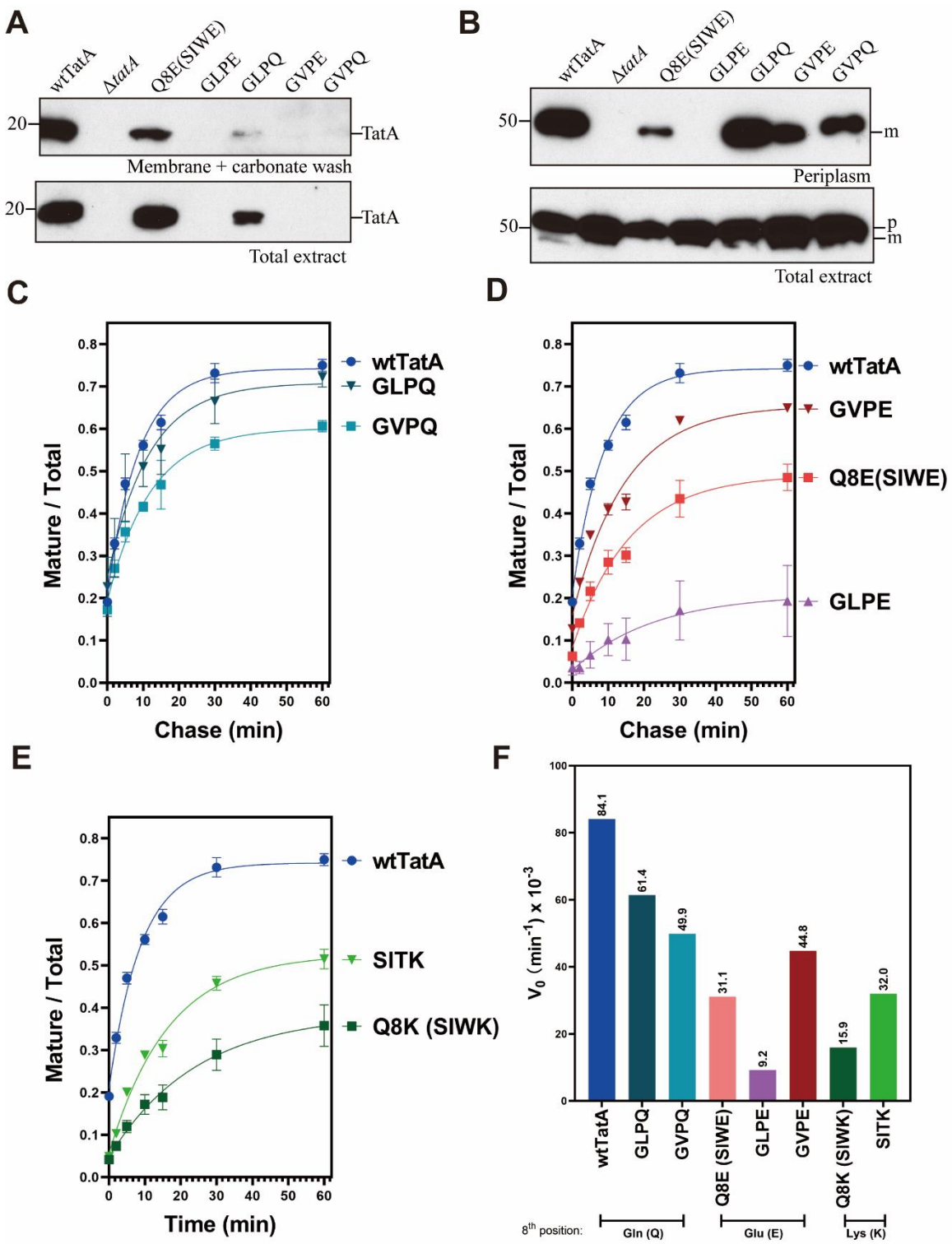

Figure 6. Comparison of the Tat transport activity with the TatA N-terminal motif mutants. (A) Membrane after carbonate washing and total extract samples were subjected to SDS-PAGE and immunoblotting with the α-TatA antibody. Molecular weight is shown on the left. (B) Periplasmic fractions (top) and total extract (bottom) of the cells in the *in vivo* transport assays were isolated. Precursor (p) and mature (m) proteins were labeled on the right, and molecular weight is shown on the left. (C-E) Plots of the transport kinetics for the N-terminal motif mutants in the pulse-

chase experiment. Same analyses were carried as described earlier. At least two replicates were included for each mutant. (F) Plot of the initial velocities (V_0) of the N-terminal motif mutants in the pulse-chase experiments. V_0 was obtained from the kinetic plots in (C-E). Same methodology was implemented as described before. Exact values of the initial velocities are displayed on top of bar graph.

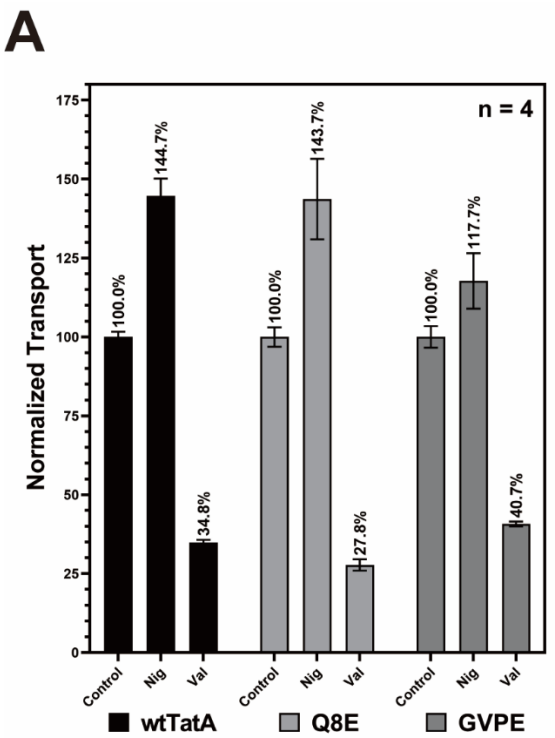

Figure 7. TatA N-terminus mutants have different behavior than wtTat in energy utilization preference and thermostability. (A) Comparison of the IMV transport of SufI among wtTatA, TatA Q8E (SIWE), and TatA GVPE mutants in response to 10 μM nigericin or 10 μM valinomycin treatment. The solvent of nigericin and valinomycin, ethanol, was used as the control group which were defined as 100% of transport in the bar graph. The exact percentage is shown on top. Each treatment group per mutant was performed in four replicates, see Supplemental Figure 4.

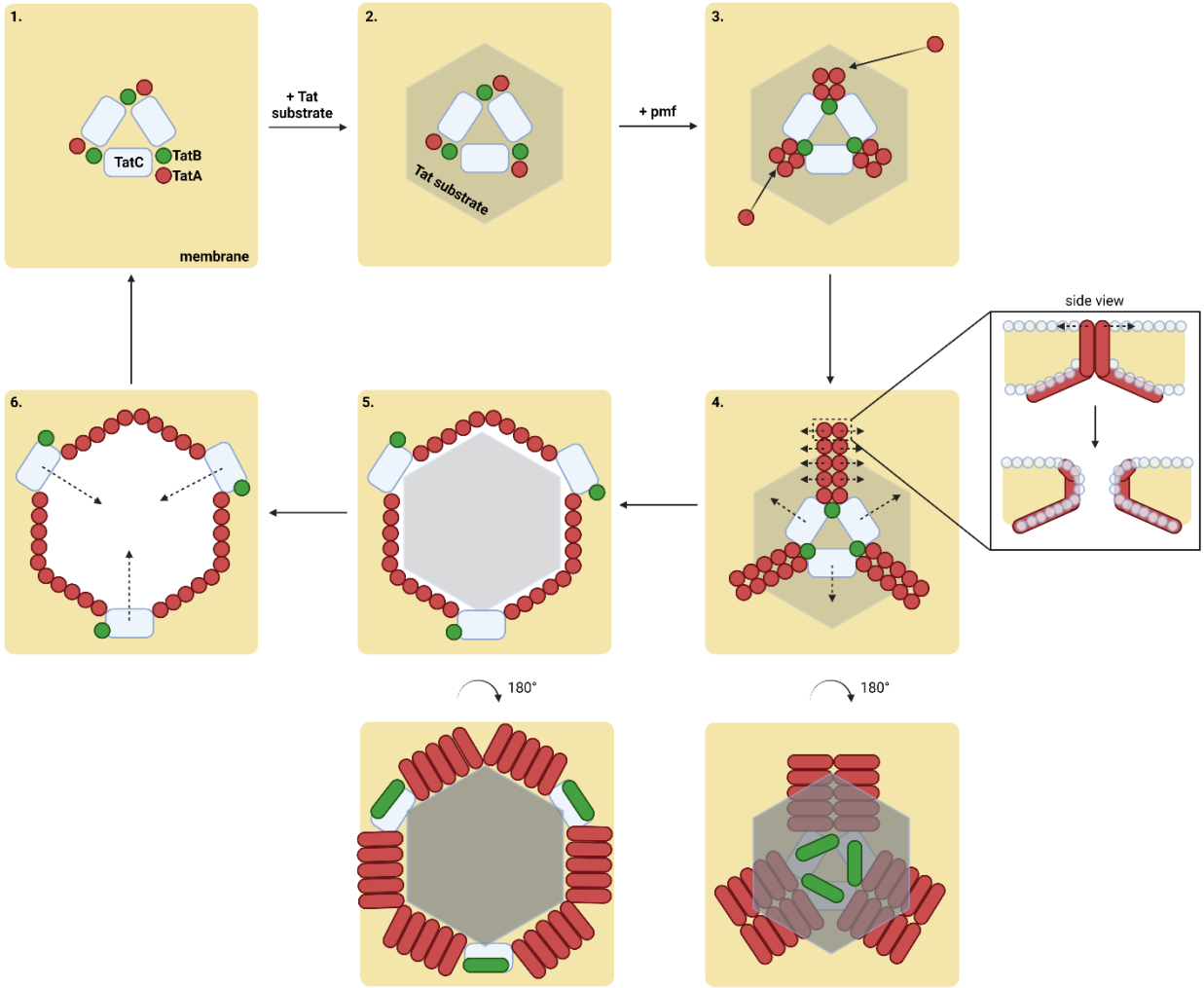

Figure 8. Schematic diagram for the proposed Tat transport mechanism. In this diagram, a top view of a proposed Tat transport process was presented. TatA, TatB and TatC proteins are shown in step 1. Side view of the TatA interfaces is shown on the right of the step 4. Blue/grey circles represent lipid head group.

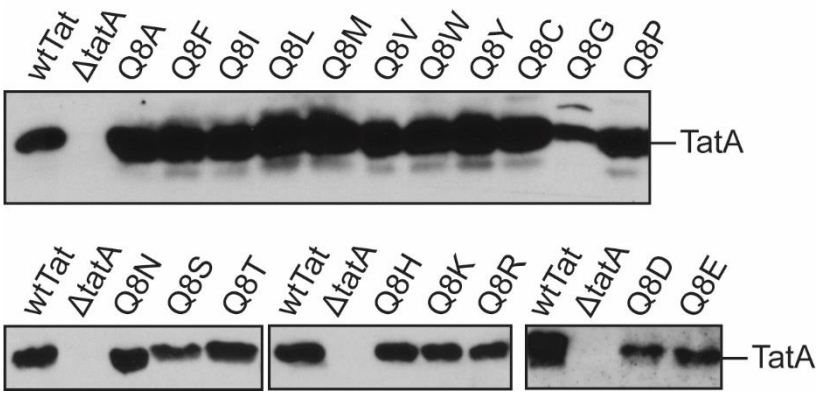

Supplemental Figure 1. Membrane stability of the TatA Q8 substituted mutants. The membrane stability of the TatA Q8 mutants together with the wtTatA and *ΔtatA* were assessed by the immunoblotting of the carbonate-treated membrane fraction from whole-cell extracts. Anti-TatA antibody was used to detect the presence of TatA in the membrane fractions.

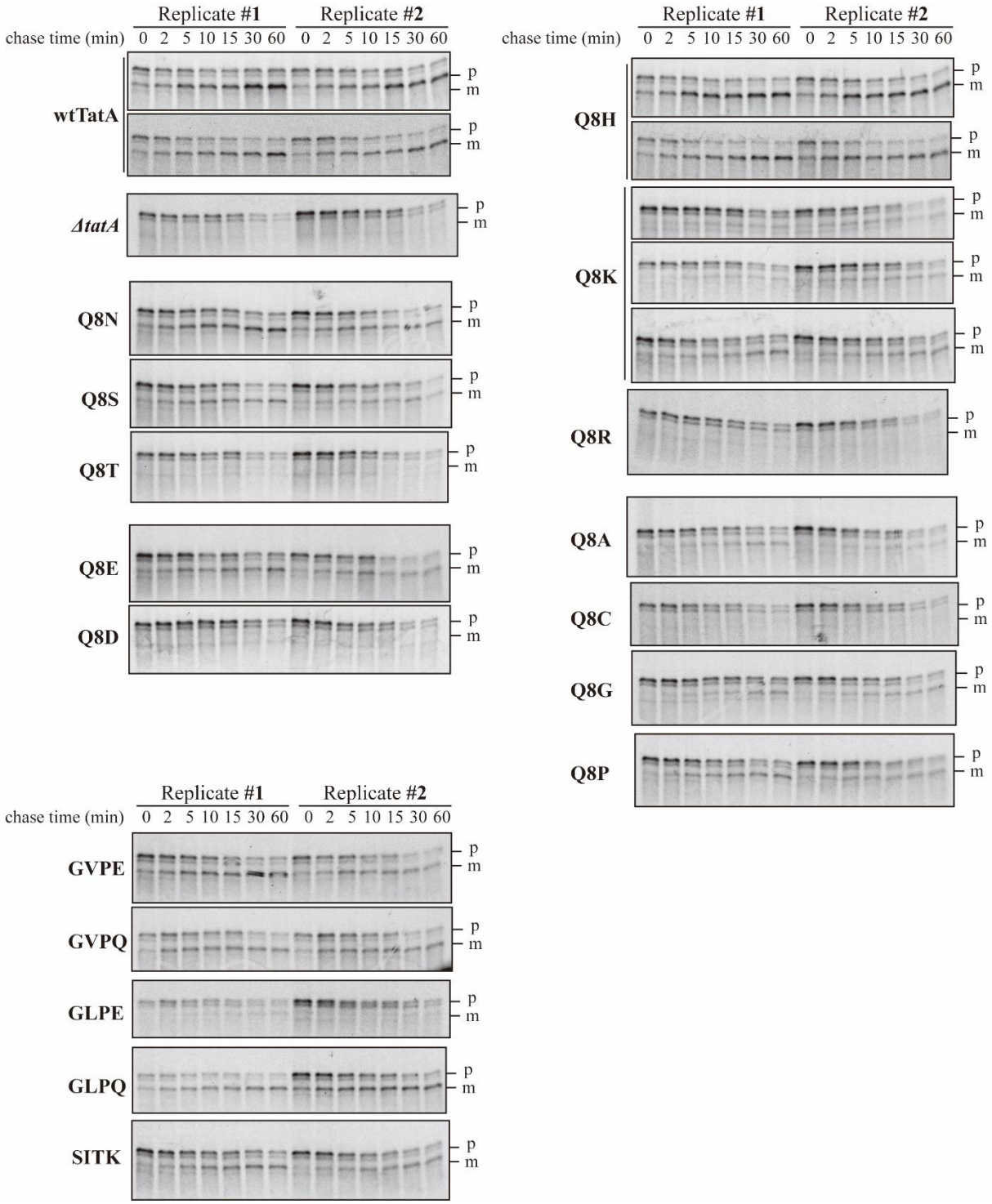

Supplemental figure 2. The autoradiography results of pulse-chase experiments. At least two replicates were performed for each mutant. Identities of the mutant is shown on the left. Replicate number and the corresponding time of chase step are shown on the top. Samples were subjected to SDS-PAGE using 8-16% polyacrylamide gels. p, precursor; m, mature.

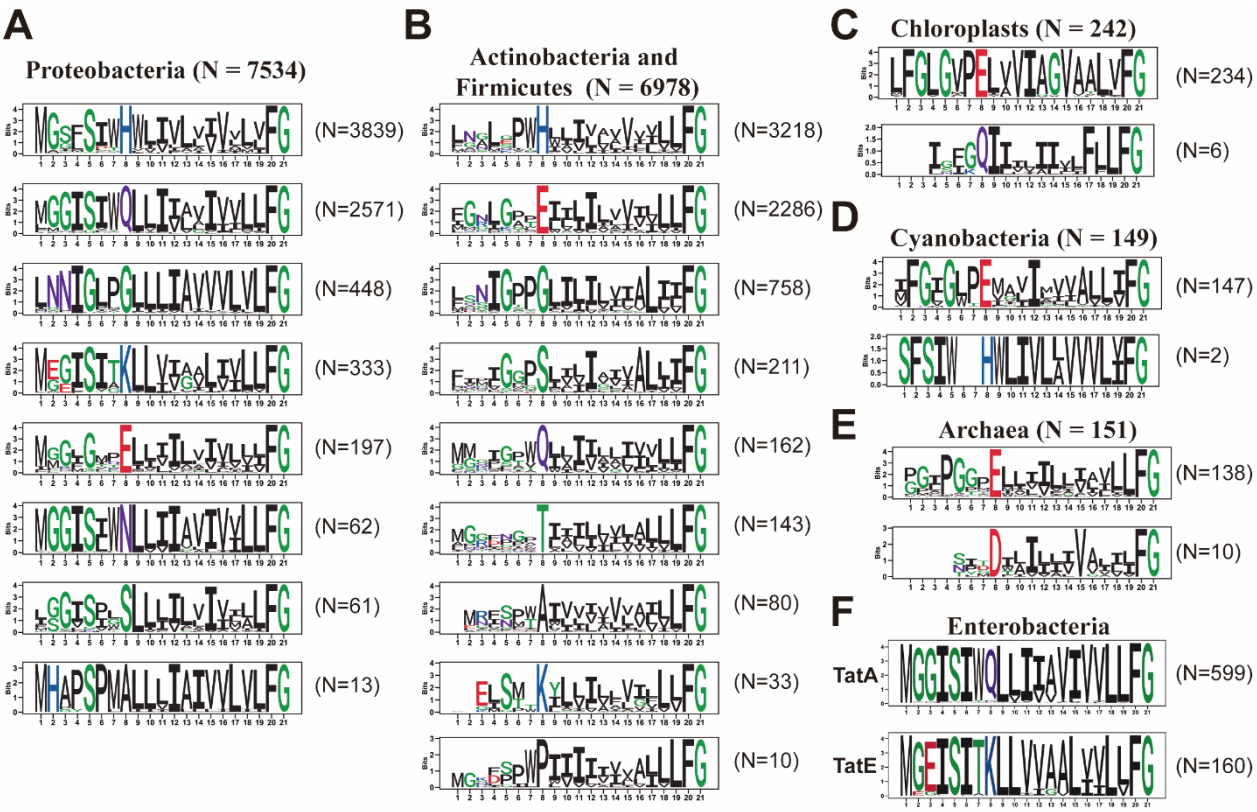

Supplemental figure 3. Detailed sequence logos across different species. Alignment data were subset based on the identity of the amino acid at the position equivalent to the eighth one in the *E. coli* TatA. N, number of sequences used to generate the sequence logo. (A) Sequence logos for proteobacteria. (B) Sequence logos for actinobacteria and firmicutes. (C) Sequence logos for chloroplasts. (D) Sequence logos for cyanobacteria. (E) Sequence logos for archaea. (F) A subset of data, enterobacteria, which possess TatE, were separated from proteobacteria to generate the sequence logos.

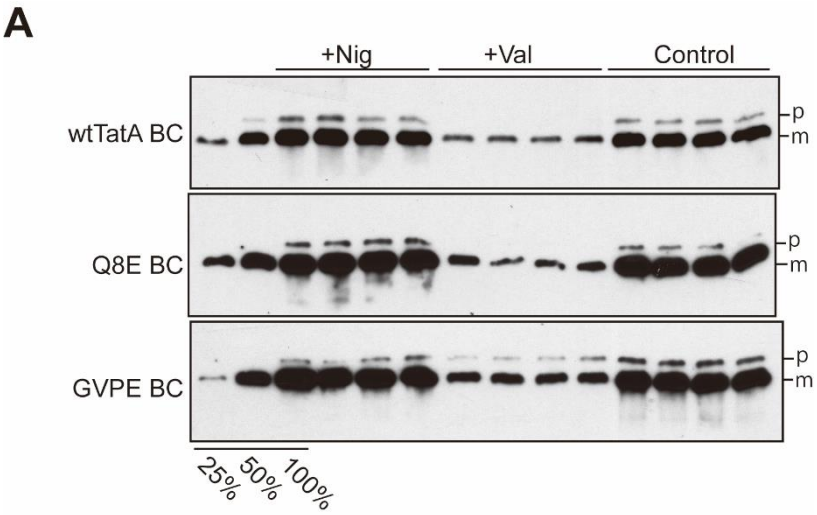

Supplemental figure 4. Western-blot results of the IMV transport assay. IMVs transporting biotinylated SufI were subjected to proteinase K digestion to remove the non-transported SufI. Digested samples were subjected to SDS-PAGE using 8-16% polyacrylamide gels followed by Western-blot using avidin to detect the biotinylated SufI. Identities of the IMVs are shown to the left. Experimental treatments are shown on the top. p, precursor; m, mature. Four replicates were included in this experiment.

Supplemental Table 1

Species name	Residue at 8th position	Living condition	Data source
Acidithrix ferrooxidans	Asp (D)	pH 1.5	(1)
Corynebacterium sp. DSM 45110	Asp (D)	n.d.	N/A
Candidatus Aramenus sulfurataquae	Asp (D)	Muddy water from acid hot spring	The data have been deposited with links to BioProject accession number PRJNA273893 in the NCBI BioProject database (https://www.ncbi.nlm.nih.gov/bioproject/).
Ferroplasma acidarmanus	Asp (D)	pH 0 - 2.5	(2)
Picrophilus torridus	Asp (D)	pH 0	(3)
Metallosphaera cuprina	Asp (D)	pH 3.5, 55 - 75°C	(4)
Ferroplasma acidiphilum	Asp (D)	pH 1.7	(5)
Picrophilus oshimae	Asp (D)	pH < 3.5, optimal pH 0.7	(6)
Sulfurisphaera ohwakuensis	Asp (D)	pH 1.0 - 5.0, optimal pH 2.0	(7)

n.d. = no data; N/A = not applicable.

1. Jones RM, Johnson DB. Acidithrix ferrooxidans gen. nov., sp. nov.; a filamentous and obligately heterotrophic, acidophilic member of the Actinobacteria that catalyzes dissimilatory oxido-reduction of iron. Res Microbiol. 2015 Mar;166(2):111–20.
2. Baumler DJ, Jeong K-C, Fox BG, Banfield JF, Kaspar CW. Sulfate requirement for heterotrophic growth of “Ferroplasma acidarmanus” strain fer1. Res Microbiol. 2005 May 1;156(4):492–8.
3. Fütterer O, Angelov A, Liesegang H, Gottschalk G, Schleper C, Schepers B, et al. Genome sequence of Picrophilus torridus and its implications for life around pH 0. Proc Natl Acad Sci. 2004 Jun 15;101(24):9091–6.
4. Liu L-J, You X-Y, Guo X, Liu S-J, Jiang C-Y 2011. Metallosphaera cuprina sp. nov., an acidothermophilic, metal-mobilizing archaeon. Int J Syst Evol Microbiol. 61(10):2395–400.
5. Golyshina OV, Pivovarova TA, Karavaiko GI, Kondratéva TF, Moore ER, Abraham WR, et al. Ferroplasma acidiphilum gen. nov., sp. nov., an acidophilic, autotrophic, ferrous-iron-oxidizing, cell-wall-lacking, mesophilic member of the Ferroplasmaceae fam. nov., comprising a distinct lineage of the Archaea. Int J Syst Evol Microbiol. 50(3):997–1006.
6. Schleper C, Puehler G, Holz I, Gambacorta A, Janekovic D, Santarius U, et al. Picrophilus gen. nov., fam. nov.: a novel aerobic, heterotrophic, thermoacidophilic genus and family comprising archaea capable of growth around pH 0. J Bacteriol. 1995 Dec 1;177(24):7050–9.
7. Kurosawa N, Itoh YH, Iwai T, Sugai A, Uda I, Kimura N, et al. Sulfurisphaera ohwakuensis gen. nov., sp. nov., a novel extremely thermophilic acidophile of the order Sulfolobales. Int J Syst Evol Microbiol. 48(2):451–6.

983 **Supplemental Table 2. Primer sequences in this study.**

Primer Name	Primer Sequence
TatA_Q8A_F	5’-CAGTATTTGGgcgTTATTGATTATTGCCGTC-3’
TatA_Q8C_F	5’-CAGTATTTGGtgcTTATTGATTATTGCCGTCATCGTTG-3’
TatA_Q8D_F	5’-CAGTATTTGGgatTTATTGATTATTGCCG -3’
TatA_Q8E_F	5’-CAGTATTTGGgagTTATTGATTATTGC-3’
TatA_Q8F_F	5’-CAGTATTTGGtttTTATTGATTATTGCCGTCATCGTTG-3’
TatA_Q8G_F	5’-CAGTATTTGGggtTTATTGATTATTGCCGTCATCG-3’
TatA_Q8H_F	5’-CAGTATTTGGcacTTATTGATTATTGCCG-3’
TatA_Q8I_F	5’-CAGTATTTGGattTTATTGATTATTGCCGTCATCG-3’
TatA_Q8K_F	5’-CAGTATTTGGaagTTATTGATTATTGC-3’
TatA_Q8L_F	5’-CAGTATTTGGctgTTATTGATTATTGC-3’
TatA_Q8M_F	5’-CAGTATTTGGatgTTATTGATTATTGCCG-3’
TatA_Q8N_F	5’-CAGTATTTGGaatTTATTGATTATTGCCGTC-3’
TatA_Q8P_F	5’-CAGTATTTGGccgTTATTGATTATTGC-3’
TatA_Q8R_F	5’-CAGTATTTGGagaTTATTGATTATTGCCGTCATCG-3’
TatA_Q8S_F	5’-CAGTATTTGGagcTTATTGATTATTGCCGTC-3’
TatA_Q8T_F	5’-CAGTATTTGGaccTTATTGATTATTGCCGTCATCG-3’
TatA_Q8V_F	5’-CAGTATTTGGgtgTTATTGATTATTGCCGTC-3’
TatA_Q8W_F	5’-CAGTATTTGGtggTTATTGATTATTGCCGTC-3’
TatA_Q8Y_F	5’-CAGTATTTGGtatTTATTGATTATTGCCGTC-3’
TatA_Q8_R	5’-ATACCACCCATGGATCCTC-3’
TatA_GLPE_F	5’-cctggaTTATTGATTATTGCCGTCATC-3’
TatA_GLPE_R	5’-aagaccGATACCACCCATGGATCC-3’
TatA_GLPQ_F	5’-accgCAGTTATTGATTATTGCCGTC-3’
TatA_GLPQ_R	5’-aaaccGATACCACCCATGGATCC-3’
TatA_GVPE_F	5’-ccggagTTATTGATTATTGCCGTCATC-3’
TatA_GVPE_R	5’-aacaccGATACCACCCATGGATCC-3’
TatA_GVPQ_F	5’-ccgcagTTATTGATTATTGCCGTCATC-3’
TatA_GVPQ_R	5’-aacaccGATACCACCCATGGATCC-3’

TatA_SITK_F	5’-accaaaTTATTGATTATTGCCGTCATC-3’
TatA_SITK_R	5’-aatactGATACCACCCATGGATCC-3’
pBAD33(TatA_Q8E)_F	5’-CAGTATTTGGgagTTATTGATTATTG-3’
pBAD33(TatA_Q8K)_F	5’-CAGTATTTGGaaaTTATTGATTATTGC-3’
pBAD33(TatA_Q8)_R	5’-ATACCACCCATGACCTTTC-3’
pBAD33(TatA_7P8E)_F	5’-ccggagTTATTGATTATTGCCGTCATC-3’
pBAD33(TatA_7P8Q)_F	5’-ccgcagTTATTGATTATTGCCGTCATC-3’
pBAD33(TatA_5G6V)_R	5’-cacgccGATACCACCCATGACCTTTC-3’
pBAD33(TatA_5G6L)_F	5’-caggccGATACCACCCATGACCTTTC -3’

Note: mutagenesis sites are shown in lowercase.

Supplemental Table 3. Plasmids information in this study.

Name	Description	Source
Vector		
pBAD22	Expression vector with arabinose-inducible *araBAD* operon, carbenicillin resistance	ATCC
pBAD33	Expression vector with arabinose-inducible *araBAD* operon, chloramphenicol resistance	(1)
pQE80l	Expression vector with IPTG-inducible T5 promoter	Qiagen
Substrate		
pNR14	*E. coli* SufI in pT7.5 vector with T7 ϕ10 promoter	(2)
pNR42	Phage T7 polymerase and the temperature-sensitive λ repressor in pSU18	(3)
pQE80l (SufI-FLAG)	*E. coli* SufI with C-terminal FLAG tag in pQE80l vector	This work
Mutant		
pTat101	pTH19Kr derivative, a low copy vector, expression of TatABC	(4)
ΔTatA	pTH19Kr derivative, a low copy vector, expression of TatBC	This work
pTat101 (Q8A)	pTat101 with Ala substitution for Gln8 in TatA	This work
pTat101 (Q8C)	pTat101 with Cys substitution for Gln8 in TatA	This work
pTat101 (Q8D)	pTat101 with Asp substitution for Gln8 in TatA	This work
pTat101 (Q8E)	pTat101 with Glu substitution for Gln8 in TatA	This work
pTat101 (Q8F)	pTat101 with Phe substitution for Gln8 in TatA	This work
pTat101 (Q8G)	pTat101 with Gly substitution for Gln8 in TatA	This work

pTat101 (Q8H)	pTat101 with His substitution for Gln8 in TatA	This work
pTat101 (Q8I)	pTat101 with Ile substitution for Gln8 in TatA	This work
pTat101 (Q8K)	pTat101 with Lys substitution for Gln8 in TatA	This work
pTat101 (Q8L)	pTat101 with Leu substitution for Gln8 in TatA	This work
pTat101 (Q8M)	pTat101 with Met substitution for Gln8 in TatA	This work
pTat101 (Q8N)	pTat101 with Asn substitution for Gln8 in TatA	This work
pTat101 (Q8P)	pTat101 with Pro substitution for Gln8 in TatA	This work
pTat101 (Q8R)	pTat101 with Arg substitution for Gln8 in TatA	This work
pTat101 (Q8S)	pTat101 with Ser substitution for Gln8 in TatA	This work
pTat101 (Q8T)	pTat101 with Thr substitution for Gln8 in TatA	This work
pTat101 (Q8V)	pTat101 with Val substitution for Gln8 in TatA	This work
pTat101 (Q8W)	pTat101 with Trp substitution for Gln8 in TatA	This work
pTat101 (Q8Y)	pTat101 with Tyr substitution for Gln8 in TatA	This work
pTat101 (Ad2)	pTat101 with Leu18 and Leu19 deletion in TatA	
pTat101 (GLPE)	pTat101 with Gly substitution for Ser5, Leu substitution for Ile6, Pro substitution for Trp7, and Glu substitution for Gln8 in TatA	This work
pTat101 (GLPQ)	pTat101 with Gly substitution for Ser5, Leu substitution for Ile6, Pro substitution for Trp7 in TatA	This work
pTat101 (GVPE)	pTat101 with Gly substitution for Ser5, Val substitution for Ile6, Pro substitution for Trp7, and Glu substitution for Gln8 in TatA	This work
pTat101 (GVPQ)	pTat101 with Gly substitution for Ser5, Val substitution for Ile6, Pro substitution for Trp7 in TatA	This work
pTat101 (SITK)	pTat101 with Thr substitution for Trp7, and Lys substitution for Gln8 in TatA	This work
pTat101 (GVPE(ACa1))	pTat101 (GVPE) with one Leu addition after Leu19 in TatA	This work
pTat101 (GVPE(ACa2))	pTat101 (GVPE) with two Leu additions after Leu19 in TatA	This work
pTat101 (GVPQ(ACa1))	pTat101 (GVPQ) with one Leu addition after Leu19 in TatA	This work
pTat101 (GVPQ(ACa2))	pTat101 (GVPQ) with two Leu additions after Leu19 in TatA	This work
pBAD22(TatABC)	TatABC in pBAD22	This work
pBAD22 (Q8E)	TatA with Glu substitution for Gln8 in pBAD22	This work
pBAD22 (Q8K)	TatA with Lys substitution for Gln8 in pBAD22	This work
pBAD22 (GLPE)	TatA with Gly substitution for Ser5, Leu substitution for Ile6, Pro substitution for Trp7, and Glu substitution for Gln8 in pBAD22	This work

pBAD22 (GLPQ)	TatA with Gly substitution for Ser5, Leu substitution for Ile6, Pro substitution for Trp7 in pBAD22	This work
pBAD22 (GVPE)	TatA with Gly substitution for Ser5, Val substitution for Ile6, Pro substitution for Trp7, and Glu substitution for Gln8 in pBAD22	This work
pBAD22 (GVPQ)	TatA with Gly substitution for Ser5, Val substitution for Ile6, Pro substitution for Trp7 in pBAD22	This work
pBAD33(TatAhis)	TatA with a C-terminal 6X His in pBAD33	This work
pBAD33 (Q8Ehis)	TatA with Glu substitution for Gln8 and a C-terminal 6X His in pBAD33	This work
pBAD33 (Q8Khis)	TatA with Lys substitution for Gln8 and a C-terminal 6X His in pBAD33	This work
pBAD33 (GLPEhis)	TatA with Gly substitution for Ser5, Leu substitution for Ile6, Pro substitution for Trp7, Glu substitution for Gln8, and a C-terminal 6X His in pBAD33	This work
pBAD33 (GLPQhis)	TatA with Gly substitution for Ser5, Leu substitution for Ile6, Pro substitution for Trp7, and a C-terminal 6X His in pBAD33	This work
pBAD33 (GVPEhis)	TatA with Gly substitution for Ser5, Val substitution for Ile6, Pro substitution for Trp7, Glu substitution for Gln8, and a C-terminal 6X His in pBAD33	This work
pBAD33 (GVPQhis)	TatA with Gly substitution for Ser5, Val substitution for Ile6, Pro substitution for Trp7, and a C-terminal 6X His in pBAD33	This work

1. L. M. Guzman, D. Belin, M. J. Carson, J. Beckwith, Tight regulation, modulation, and high-level expression by vectors containing the arabinose PBAD promoter. *Journal of Bacteriology* **177**, 4121–4130 (1995).
2. N. R. Stanley, T. Palmer, B. C. Berks, The twin arginine consensus motif of Tat signal peptides is involved in Sec-independent protein targeting in Escherichia coli. *Journal of Biological Chemistry* **275**, 11591–11596 (2000).
3. F. Sargent, N. R. Stanley, B. C. Berks, T. Palmer, Sec-independent Protein Translocation in Escherichia coli. *Journal of Biological Chemistry* **274**, 36073–36082 (1999).
4. H. Kneuper, *et al.*, Molecular dissection of TatC defines critical regions essential for protein transport and a TatB–TatC contact site. *Molecular Microbiology* **85**, 945–961 (2012).